INCORPORATING SHRINKAGE EFFECTS IN FE MODELING OF PRESTRESSED CONCRETE BRIDGE

By

DHARA PURANI

A thesis submitted to the

Graduate School-New Brunswick

Rutgers, The State University of New Jersey

in partial fulfillment of the requirements

for the degree of

Master of Science

Graduate Program in Civil and Environmental Engineering

written under the direction of

Dr. Hani H. Nassif

and approved by

_____

_____

_____

New Brunswick, New Jersey

May, 2013

ABSTRACT OF THE THESIS

INCORPORATING SHRINKAGE EFFECTS IN FE MODELING OF

PRESTRESSED CONCRETE BRIDGE

By DHARA PURANI

Thesis Director:

Dr. Hani H. Nassif

Right from the inception of the implementation of prestressed concrete in the bridge construction field, it has been very popular. Even though this type of bridges has big advantages, cracking is a major problem. The cracking event, due to its detrimental effects on the structure is the most objectionable problem. In cracking shrinkage plays a very significant role. This implies that the study of shrinkage is essential to study the phenomenon of cracking. Due to many variables responsible for deck cracking, it is very difficult to study the overall effect of these variegated factors taken in the consideration at a time. This thesis aims to confluence as many such aspects as possible in a single plane of consideration with the help of Finite Element software namely ABAQUS. The goal of this research is to study shrinkage, shrinkage effects, and factors affecting the shrinkage and ultimately to incorporate the shrinkage effects in Finite Element Modeling. Here the study is constrained to Prestressed Concrete Bridge. Thus, the research is carried to incorporate the shrinkage effects in FE Modeling of Prestressed Concrete Bridge.

This is a difficult task as many finite element programs do not have pre-programmed methods for simulating the time dependent properties of concrete. Therefore, it is necessary to develop these methods. This study concentrates on trying to simulate the behavior of a simple span bridge as a means of developing the basic analytical method. In the research Abaqus has been selected and the selection has been justified for the purpose of analyzing time dependent effects in bridges. A parametric study has been carried out with a view to identifying the effects of various parameters of shrinkage in a structure. The effects of the parameters such as length of the span, girder spacing, deck thickness and modulus of elasticity of girder have been analyzed with the help of bridges modeled in Abaqus. The parametric study concludes that shrinkage strain increases with increase in length and spacing of girder. The shrinkage strain decreases with increase in compressive strength of girder and deck thickness.

ACKNOWLEDGEMENTS

I am very much grateful to many people who directly or indirectly helped me to carry my research and develop this thesis report. Foremost I feel highly indebted to Prof Hani Nassif for his constant help, encouragement and inspiration to proceed in this research work and also in writing this report. The academic as well as financial support provided by Prof Hani Nassif spawned much needed energy and motivation to attain the success with this research. I sincerely thank Dan Su for his supervisions. I am pleased to have constant guidance of my seniors Ope, Ye, Chaekuk, Yingjie and continuous help of my colleagues Miguel, Michel and Cliff. Due to their support I feel the sense of achievement and pride.

I would like to thank my father Mr. Nilesh Purani and mother Ms. Pragna Purani for having infinite faith in me and my abilities to carry my work forward. I am also very thankful to my grandfather Mr. L. J Purani for his invaluable blessings and guidance. I feel truly grateful to my brother Jitayu Purani for his never ending companionship and patience for me and my work. This work would not have been what it is today without Mr. Mukesh Bhatt and Ms. Sucheta Bhatt who made me feel comfortable living here.

TABLE OF CONTENT

ABSTRACT OF THESIS ii

ACKNOWLEDGEMENTS iv

1 INTRODUCTION 1

1.1 GENERAL 1

1.2 BRIDGE DECK CRACKING 2

1.2.1 SHRINKAGE 4

1.2.2 CREEP 5

1.2.3 THERMAL EFFECTS 7

1.2.4 RESTRAINT 9

1.3 LITERATURE REVIEW 12

1.4 OBJECTIVE OF RESEARCH 29

2 SHRINKAGE MODELS 30

2.1 SHRINKAGE 30

2.2 TYPES OF SHRINKAGE 31

2.2.1 PLASTIC SHRINKAGE 32

2.2.2 THERMAL SHRINKAGE 33

2.2.3 AUTOGENOUS SHRINKAGE 34

2.2.4 DRYING SHRINKAGE 36

2.3 SHRINKAGE PREDICTION EQUATION 37

2.4 INCORPORATING SHRINKAGE INTO FE 41

3 FINITE ELEMENT MODEL VALIDATION 46

3.1 DESIGN OF BRIDGE (P/C) AND DATA BASE 46

3.1.1 DESIGN OF BRIDGE (P/C) 46
3.1.2 DATABASE FOR PARAMETRIC STUDY 48
3.2 MODEL DESCRIPTION 51
3.2.1 INTRODUCTION 51
3.2.2 GEOMETRIC MODELLING 52
3.2.3 MATERIAL PROPERTIES 56
3.2.4 LOADING 56
3.3 COMPARISION WITH FIELD DATA 57
4 RESULTS 65
4.1 RESULT OF BRIDGE 65
4.2 PARAMETRIC STUDY RESULTS 67
5 CONCLUSIONS 82
5.1 CONCLUSIONS 82
5.2 FUTURE INVESTIGATION 84
REFERENCES 85
APPENDIX 87

LIST OF FIGURES

Figure 1: Causes of bridge deck cracking 4

Figure 2: Bridge B-20-133/134 13

Figure 3: Longitudinal stress Contour on Top of Deck from Shrinkage analysis 14

Figure 4: Transverse stress contour on top of deck from Shrinkage Analysis 15

Figure 5: Bridge over Newfound River 17

Figure 6: Comparison of Abaqus and FHWA data 18

Figure 7: FE mesh of the three girder bridge 20

Figure 8: Transverse Strain Distribution 20

Figure 9: Longitudinal Strain Distribution 21

Figure 10: View of Span A and Location of Applied Loads 23

Figure 11: Transverse strain at Top Surface of Deck 24

Figure 12: Transeverse strain at Bottom surfsce of deck 24

Figure 13: Computed temperature at node 16 corresponding to location of gage T9 26

Figure 14: Thermal Expansion Strains during hydration of concrete 27

Figure 15: Computed Residual Stresses in Concrete at the bottom of the deck due to Temperature and Shrinkage 27

Figure 16: Girder of Bridge 1 48

Figure 17: Integration points of two-node linear beam B31 53

Figure 18: Integration points of a four-node shell element (Abaqus) 54

Figure 19: Integration points on I section 55

Figure 20: Cross Section of the Bridge 58

Figure 21: Validation bridge model with single girder 59

Figure 22: Profile of girder 61

Figure 23: Stress in the Deck 62

Figure 24: Strain Data from FHWA observations 63

Figure 25: Comparison graph with field data 64

Figure 26: Abaqus model of Bridge 1 65

Figure 27: Abaqus Model of Bridge 1 with single girder 65

Figure 28: Stress in top of the deck 66

Figure 29: Stress in bottom of the deck 66

Figure 30: Shrinkage in girder 66

Figure 31: Stress in top of the deck 67

Figure 32: Stress in bottom of the deck 67

Figure 33: Stress at top of the Deck for 80 ft span 68

Figure 34: Shrinkage in top of the Deck for 80 ft span 68

Figure 35: Stress in top of the Deck for 100 ft span..... 68

Figure 36: Shrinkage in top of the Deck for 100 ft span 69

Figure 37: Comparison of Strain in girders for span length 80 ft and 100 ft 69

Figure 38: Stress in top of the deck for 60 ft span..... 70

Figure 39: Shrinkage strain in top of the deck for 60 ft span 70

Figure 40: Stress in top of the deck for 80 ft span..... 70

Figure 41: Shrinkage in top of the deck for 80 ft span..... 71

Figure 42: Comparison of Strain in girders for span length 60 ft and 80 ft 71

Figure 43: Stress in top of the deck for 6 ft spacing of girder..... 72

Figure 44: Shrinkage in top of the deck for 6 ft spacing of girder 72

Figure 45: Stress in top of the deck for 8 ft spacing of girder..... 72

Figure 46: Shrinkage in top of the deck for 8 ft spacing of girder 73

Figure 47: Stress in top of the deck for 10 ft spacing of girder..... 73

Figure 48: Shrinkage in top of the deck for 10 ft spacing of girder 73

Figure 49: Comparison of Strain in girders for girder spacing of 6 ft, 8 ft and 10 ft..... 74

Figure 50: Stress in top of the deck for 6 in thickness of deck 75

Figure 51: Shrinkage in top of the deck for 6 in thickness of deck 75

Figure 52: Stress in top of the deck for 8 in thickness of deck 75

Figure 53: Shrinkage in top of the deck for 8 in thickness of deck 75

Figure 54: Stress in top of the deck for 10 in thickness of deck 76

Figure 55: Shrinkage in top of the deck for 10 in thickness of deck 76

Figure 56: Comparison of Strain in girders with deck thickness of 6 in, 8 in and 10 in 77

Figure 57: Stress in top of the deck for 6 ksi compressive strength 78

Figure 58: Shrinkage in top of the deck for 6 ksi compressive strength 78

Figure 59: Stress in top of the deck for 8 ksi compressive strength 78

Figure 60: Shrinkage in top of the deck for 8 ksi compressive strength 78

Figure 61: Stress in top of the deck for 10 ksi compressive strength 79

Figure 62: Shrinkage in top of the deck for 10 ksi compressive strength 79

Figure 63: Comparison of Strain in girders for compressive strength of 6 ksi, 8 ksi and 10 ksi 80

Figure 64: Shrinkage strain in top of the deck with pinned –roller boundary condition 80

Figure 65: Shrinkage strain in top of the deck with pinned –pinned boundary condition 81

Figure 66: Shrinkage strain in top of the deck with fixed –fixed boundary condition 81

LIST OF TABLES

Table 1: Strand Patterns of Bridge 1 48

Table 2: Bridges for Parametric Study with respect to Length 49

Table 3: Bridges for Parametric Study with respect to Girder Spacing 50

Table 4: Bridges for Parametric Study with respect to Deck Thickness..... 50

Table 5: Bridges for Parametric Study with respect to Compressive strength of the Girder f'c ... 51

Table 6: Bridges for Parametric Study with respect to restrained conditions..... 51

Table 7: Modified Strand Pattern 59

Table 8: Variation of E with respect to Age of Girder 60

Table 9: Variation of E with respect to Age (Deck) 60

CHAPTER 1

Introduction

1.1 General

The implementation of the prestressed concrete in bridge building came into effect around 1950. From then onwards the concept has been in use extensively because of structural and commercial advantages it provides (PCI 2004). It has also been noted by TRB that more than 20% of bridge in USA inventory of the aforesaid type and in addition to it in the upcoming bridges those are being built more than 50% are of this type (TRB 2000). Bridge decks have many problems with cracking. The cracking plays primary role in the wearing off the bridge decks. It deteriorates the decks and cause significant damage. It is very relevant to note the fact that in totality more than 100k bridge decks which comprises almost half of the total bridges of USA suffer from transverse cracking at initial age (Krauss and Rogalla, 1996).

For understanding the significance of the cracking problem, we can refer to some of the surveys conducted by various state authorities. NYSDOT conducted a survey for New York State on around 63 bridges in northern region of the state and it was found that merely 15 bridges had not suffered from deck cracking. In an another research it was found out that nearly 40% of the single-span bridges and nearly 70% of multiple spans bridges developed considerable cracking on the concrete deck (Curtis and White 2007). Similar result was obtained for the Wisconsin state. There has been noted a tendency in new bridge decks of developing transverse cracking. There are numerous reasons associated with development of transverse cracking such as constitutional properties, method of construction and structural configuration. The

developments of cracks have been reported from almost all the states of the country. The concrete properties of the decks have been identified as the main culprit that holds the responsibility of including cracking.

The reports by the State Highways Agencies also mark this early or initial age cracking as universal problem for decks. For the records it is worthwhile to note that 97% of states Departments of Transportation raise their concerns with this early age cracking (Aktan et al., 2003). A number of studies that has been performed to evaluate and analyze roots and phenomenon of early age cracking quarantine some of the main reasons for the cracking. Some of these causes/roots are thermal movement, early age shrinkage and early age settlement (Krauss and Rogalla, 1996; Babaei, 2005). Some of the reasons for cracking include shrinkage while curing, temperature alterations, lack of satisfactory support, magnification of applied loads and restraint conditions. Early age cracking decreases the functional life of the structures which is a serious problem. In a study carried by Jason lee meadows, it has been noted that the actual mechanism is based on various factors that are very difficult and intricate to be analyzed effectively.

1.2 Bridge Deck Cracking

This segment covers the conclusions and findings of extensive literature review related to Bridge Deck Cracking. These include the causes, mechanisms related and phenomenon of the Cracking. This chapter serves as a synopsis to the literature review and justifies the significance and importance of the enormous research done on concrete cracking event. As noted in the previous section the problem is found in and recognized as a major problem by almost every

state of the USA. The transportation authorities of several states (Department of Transportation DOT) and National Authority (National Cooperative Highway Research Program NCHRP) have conducted various surveys, studies and researches on it and their reviews have been documented comprehensively. These reports identify and could analyze the problems statistically. It also concluded some of the variables that are directly related to the problem. It has been reported that the after the late 1980's, the occurrence of early age cracks in concrete bridge decks has increased considerably. One such conclusion also emphasizes the fact that these cracks might take place even before structure is opened for traffic. In some of the cases this occurred right after the construction was completed (Schmitt and Darwin 1995; Saadeghvaziri and Hadidi 2002). A research project of Department of Transportation (DOT) of 1996 concluded that around 42% bridges suffer from cracking in very first week after it has been built (Krauss and Rogalla 1996).

In a comprehensive study carried in 2007, Curtis and White concluded a few of the most powerful factors which hold tremendous effect on cracking phenomenon. These are namely 1) The concrete Strength 2) The concrete cover thickness above the reinforcing steel 3) The pouring temperature of concrete. The tensile stresses induced during/due to events such as concrete shrinkage, temperature variations in the concrete material, dead and live loads (i.e. self-weight and traffic loads) determine or govern the phenomenon of cracking. The reason stresses are induced in bridge decks is restraint provided by the girders. These girders hinder thermal and shrinkage movements of the deck due to their inherent difference in responding the action. This converts strain into stresses. Considerable contribution has come from Brown et al. (2001) in identifying the mechanical reasons for bridge deck cracking.

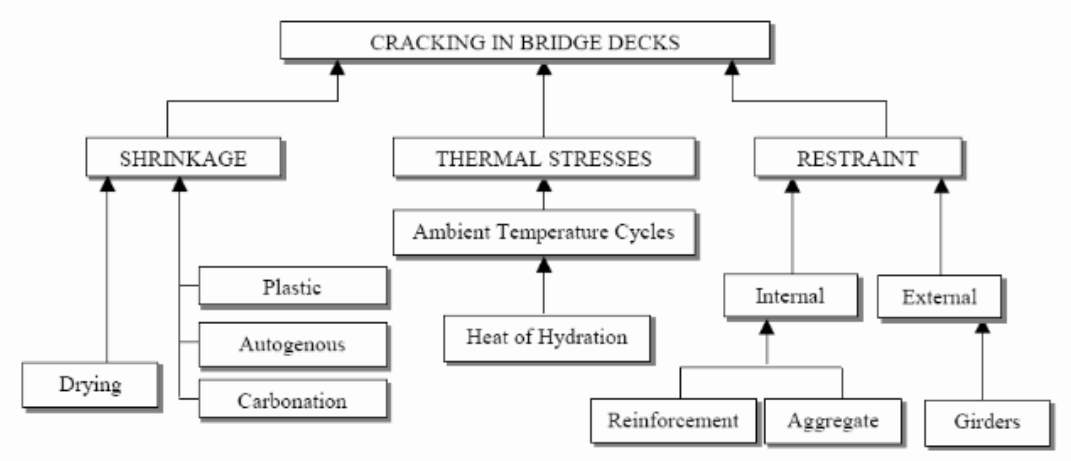

Figure 1: Causes of bridge deck cracking (Brown, et al., 2001)

As seen in this figure, Brown et al. consider shrinkage, thermal stresses, and restraint to be the primary factors in cracking. Each of these factors is an event needed to be evaluated carefully for analyzing the cracking phenomenon.

1.2.1 Shrinkage

The shrinkage has been identified as the principal cause of strain in concrete bridge deck. It is worthy to note that the intensity of the shrinkage can be so high that it can alone produce cracks in concrete even without the presence of temperature/thermal stains (Krauss and Rogalla, 1996). Cracking takes place when moisture and temperature alterations stimulate volumetric alterations of restrained portion of the concrete. The foremost reason of the transverse deck cracking as recognized by the Division of Research at the Indiana Department of Transportation is hindrance to concrete shrinkage of bridge decks (Frosch 2003). During casting, concrete has to face changes in volumetric identities such as size and shape. These are imparted even when there is no physical loading applied. These modifications in size are mainly due to concrete shrinkage. Thus the changes in volumetric entities are due to shrinkage. Shrinkage in

turn is due to moisture evaporation and chemical processes between changing constituents of the concrete.

It should be noted that the volumetric changes identified as a major event in cracking phenomenon occur because of five types of processes namely autogenous shrinkage, drying shrinkage, thermal shrinkage, and creep. The first four represents four types of shrinkages. Out of these four, Plastic shrinkage takes place at the very beginning, at the time somewhat before the concrete is hardened. Plastic shrinkage is mainly an outcome of evaporation of water which can generate intense capillary stresses. This evaporation process is set up by poor curing conditions. If plastic shrinkage is due to loss of water in evaporation process, the autogenous shrinkage is due to loss during chemical consumption. This chemical process involves setting of chemical reactions and formation of crystal structure. Unlike these two types of shrinkages, drying shrinkage is sustained type of shrinkage and it is a long term phenomenon. In fact this shrinkage is main long term shrinkage type. The drying shrinkage too is defined by loss of water. There is one more term associated with long term shrinkage which is Carbonation shrinkage. But this type of shrinkage takes place only when there is a significant amount of CO_2 present in the surrounding air.

1.2.2 Creep

The word creep is often called Stress relaxation. This is because it is associated with the fact that this event decreases the stresses induced in the concrete. The Creep phenomenon too similar to the cracking of concrete has been studied thoroughly by researchers. Altoubat and Lange (2002) in their analysis noted that the creep is such a powerful and beneficial event that it can actually

half the shrinkage stresses. This means the reduction in the shrinkage stresses thanks to creep can be as much as 50%.

The concrete deck when subjected to prolonged loading for considerable time stimulates the creep. Creep has been classified in two categories 1) Basic Creep and 2) Drying creep. The former one takes place due to mobility of moisture with respect to surrounding environment. While the later one as name suggests is due to drying process which takes place. The drying creep is sometimes identified as an additional creep that complements the Basic creep. Even though various studies and researches have defined creep very appropriately, the term has not been quantified yet. This is mainly because of the difficulty in differentiating two strains that are involved. These are namely instantaneous strain and time dependent strain. The disparity between basic and drying shrinkage too contribute in making quantification of creep difficult (Linford and Reaveley, 2004).

As creep is also known as stress relaxation reduces the induced stresses. The phenomenon is of great interest for engineers to extract maximum advantages out of the process. Due to these facts numerous studies have been done for the same purpose. Under the effect of prolonged loading or say stresses, creep deforms the base concrete. The deformation in turn actually helps in reducing the cracking on the concrete deck. It is relevant at this point of discussion to note that the higher water-cement ratio in the concrete, low strength and soft matrix of aggregates implies high creep (Saadeghvaziri and Hadidi 2002). It is of immense importance to realize that prediction of creep reducing cracking at the early age will not hold true. This is obvious because the creep phenomenon is a long term time dependent effect. Thus creep will not be helpful for cracks appearing in immediate months after casting is done.

Even after considering above fact, results have shown that creep has to be considered as one of the most powerful tool for engineer because it draws out and nullifies most of the strains that result from hydration process and increase in the temperature that simultaneously takes place (Krauss and Rogalla 1996). There is also a danger that needs to be considered very carefully while taking use of creep. If the concrete is produced with the sole aim of fostering creep, it will go against the purpose of reducing stresses. Although as noted by Krauss and Rogalla (1996), creep has to be identified as one of the most powerful variable that can be used with a great effect in bridge deck cracking problems.

1.2.3 Thermal Effects

In case of cracking of concrete deck, apart from shrinkage effects, thermal effects are the most important factor to be considered in analysis. These effects leave a little room for engineers to work upon as they are not controllable in most of the cases. The studies show that even in the absence of shrinkage, thermal changes itself can induce cracking. The studies and researches have already confirmed the ability of thermal stresses alone to force the crack generation (Krauss and Rogalla, 1996; Aktan et al., 2003). The thermal conditions of the time just after settling of concrete is controllable and engineers can work on that for rectifying any problems. But once concrete is settled any subsequent temperature variations that ultimately impart strain cannot be controlled. This stress free condition is obtained at the time of settling of concrete. The restraint principle also applies in temperature effects, meaning if structure is restrained the conversion of strain into stress will take place unavoidably. In addition to this temperature strain, difference in the rate of contraction and expansion between support and structure (in our case girders and deck) leads to generation of differential stresses.

Some events make it extremely difficult to control the thermal effects or in other words consequence of the thermal changes. After concrete has been cured, temperature changes due to various reasons. The bridge deck undergoes seasonal variations & daily transitions in temperatures, loss of heat in hydration and also the natural solar radiation process. Aforesaid processes cause considerable temperature movements, which are governed by coefficient of thermal expansion of the concrete. In a nut shell the temperature of concrete faces significant changes because of heat of hydration due to curing process and because of environmental variations.

After concrete is placed, hydration process causes the temperature of the concrete to rise. Simultaneously the curing process also causes increase in the modulus of elasticity of the concrete. While heat of hydration process taking place if concrete is restrained, following cooling process induces tensile stresses in the concrete (Saadeghvaziri and Hadidi 2002). The note should be taken that if hardening of concrete is done at a warmer ambience; early thermal stresses are enhanced (Krauss and Rogalla 1996). Cooling concrete tries to attain the surrounding temperature. This eventually restricts the movement of elements which leads to cracking. Researchers have found that it is advisable to protect concrete from thermal contraction by covering concrete and slowing down the cooling speed (Schmitt and Darwin 1995).

The explained phenomenon follows fundamental principle of restraint. If a given volume or mass is constrained or restricted by some means from proceeding a natural equilibrant event, stresses are induced. As we are focusing on bridge deck, we can analogize that when subjected to temperature variations; it undergoes linear uniform alterations in volume across thickness of

the deck. For a specific case of solar radiation, the top surface faces maximum heat transfer compared to any other portion of the deck. This means the volumetric changes will be maximum for this top surface compared to other regions. Thus the concrete deck is subjected to restraints provided internally by difference in rate of expansion & contraction among various layers of deck thickness. This suggests that even when external restraint is not there, there can be induced thermal stresses due to internal restraints.

1.2.4 Restraint

Apart from all the sources of the strain discussed above, the sources of strain in the structure are loads. Both dead as well as live load coupled with framework deflection issues are responsible for strains in the structures. In addition to it, if volumetric alterations within the concrete are bound or hindered, indirect loading acts as an effect of it. These kinds of restraints owe presence to supportive elements such as girders, shear studs, reinforcement and also abutments (Schmitt and Darwin 1995). It is very obvious that if there is no hindrance or confrontation, strain would not be translated into stresses. And the strain induced will be limited to generating movements of the concrete. Thus the induced strains do not promote or produce cracking in the cracking. But when the system is constrained, the conversion of strain into stresses take place and this in turn generates cracking. This statement needs special attention as bridges in practical use are definitely subjected to constraints. . The case of bridge deck is highly restrained and internal as well as external restraints are inevitable. This means the conversion of strain into stresses are also inevitable. The translation process of strains into stresses is largely governed by modulus of elasticity of the concrete material. The restraints have been classified in two categories depending upon their nature: 1) Internal Restraint 2) External Restraint.

The former one is provided by bridge reinforcement, deck aggregate, and any fibers of bridge deck material. Events such as shrinkage induced from differences in the rate of losing moisture and temperature gradients along the thickness of concrete deck, serve as internal restraints in providing indirect loading. When restraint is disparate along the height of concrete deck, tensile and compressive stresses get distributed accordingly. Generally tensile stresses are placed at the surface of the deck while compressive stresses settle at the inner region of the concrete thickness (PCA 1970).

The second type of restraint is external restraint. This constraint is provided by external supportive elements or members such as girders, end supports, end restraints. In case of external restraints, any volume alterations that take place are confronted at various locations. This means the tensile stresses induced cannot find a way to be relaxed and thus over the time it stiffens up unlike in case of free shrinkage (Grasley 2003). Usual method to prevent the translation of strain into stresses is to provide expansion joints, which takes care of the movements and deflection up to certain limits without interrupting the performance of the deck. This method helps lessening external restraints and hence reduces the stresses induced.

If the girders and deck are composite, almost whole fraction of the restraint is offered by girder only (Krauss and Rogalla, 1996, Brown et al., 2001). The composite action occurs between girders and deck. This action causes deck to be subjected to the restraints. This restraint to deck's deflection translates induced strains into stresses. As emphasized earlier also, this conversion is governed by modulus of elasticity of the concrete material. In practical application of bridge decks, it is definite that girder which holds deck will be main provider of external

restraint. The rates of shrinkage of girders and deck can never be same. And this disparity implies there will be restraint by girder. If both elements are fabricated out of a single material at a time, then this inequality can be nullified. But this is not true for practical purposes. Thus girder will restrain the bottom most surface if the laying deck bed and this will hamper the movement of deck. The confrontation of the bottom surface of the deck causes eccentric restraint on the deck, which induces bending as well as planar stresses in it (Krauss and Rogalla 1996).

The shrinking of concrete generates tensile stresses in the direction of axis of the deck. Theses stresses are induced thanks to external restraint of the girder and internal restraint of the reinforcement and aggregates. The moment induced stresses overpower the tensile strength of the concrete cracks are generated starting from bottom surface to top surface. The deck cracking problem increases manifolds when the bridge is of continuous beam type or of beam with fixed ends type. In this case loading on the deck generates negative moments which complement the shrinkage stresses and in turn accentuates the cracking problem. It is to be noted that the combination of these stresses is responsible for the deterioration.

The deck crack problem has become very critical for myriads of bridges of United States of America. The process of crack generation can be briefed as follows. Bridge deck is subjected to strain that has been induced by shrinkage coupled with thermal movement and deflections. Unrestrained structure does not induce stress but restrained one translates strain into stress. These restraints are provided by the girders and the reinforcement. Concrete creep acts as stress relieving event and weakens the induced stress. It is difficult to quantify the creep. The

deck geometry too contributes to the phenomenon by changing the stress field. The tensile strength and stresses of the concrete finally determines the induction of cracking.

In a nut shell, designing prestressed concrete structures requires a lot of attention to be given to shrinkage and creep due to their influence on cracking. For accounting all the properties and their effects, it is mandatory to craft a thorough finite element shrinkage analysis code. Analysis and examination of other minor factors affecting these two chief factors and their incorporation in FEM model will provide a reliable evaluation which can be validated by experimental data.

1.3 Literature Review

The explanations and events written above necessitate analysis of tensile stresses in a bridge deck so that evaluation of the major causes of deck cracking can be done properly. It has been found that in case of prestressed concrete structures, the deck cracking induced due to shrinkage has neither been analyzed nor been evaluated perfectly. Moreover the case of strains induced because of combined effect of shrinkage and loading has never been evaluated in total sense. So for quantifying the propensity for shrinkage and load induced strains and hence stresses, to generate cracks in concrete in prestressed concrete bridges, Finite Element Simulation is needed. We have in this segment of the report included some papers which were referred to largely.

1. “Concrete Cracking in New Bridge Decks and Overlays” by Baolin Wan, Christopher Foleyand and Jordan Komp (2010)

The bridge structure B-20-133/134 of Waupun situated in Wisconsin as shown in figure 2 is a numerical model of discussed mater. ANSYS was used as an FEM tool for the analysis. 2D link elements were used for crafting rebar & steel diaphragms and 3 D brick elements were used for bearing plates, girders, barriers, concrete diaphragms and the concrete deck. The model was developed using mentioned tools (Komp 2009). It was found that each trial run was linear elastic and also it needs to be noted that results obtained from finite element simulation was based on Nodal Solutions. This linear elastic evaluation was done till there appeared first signs of cracking. In the model, the first cracking was defined by denoting a situation at which maximum tensile stress in the concrete deck exceeded the modulus of rupture of the concrete.

Figure 2: Bridge B-20-133/134 (Komp, 2010)

It should be clarified that the finite element model considered here was based on many assumptions that can simplify the problem statement. Some of these assumptions were that of neglecting mild steel reinforcement, self-weight of the bridge and removal of the bridge

barriers. Figure 3 represents the longitudinal stress contour in the concrete deck induced because of concrete shrinkage at piers. Z directional stresses obtained with the help of this FE model is helpful in obtaining various observations. It can be concluded that initially there is an increase in stress over the girders. The observation needed to be noted is that the five points located directly on the girders have nearly 15% additional stress compared to four point that are situated in between the girder spacing. This fact is very obvious as girders are source of restraint to any alterations to volume and therefore induced stress will be more.

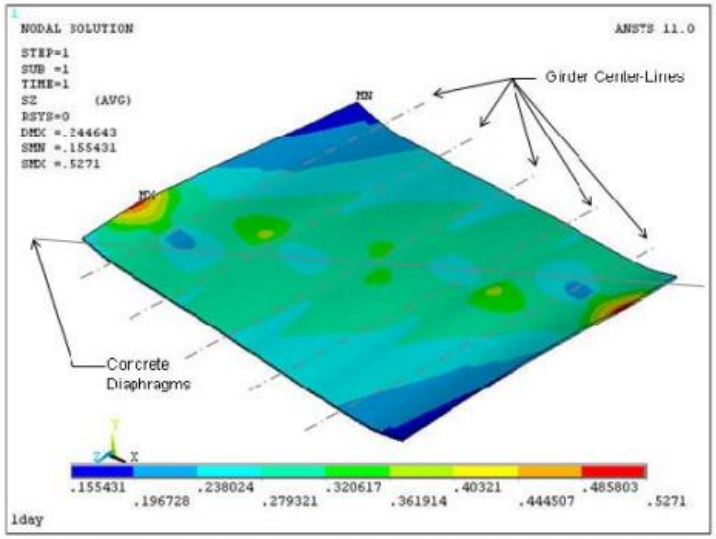

Figure 3: Longitudinal stress Contour on Top of Deck from Shrinkage analysis (Komp,2010)

Even though the trials carried were meant to determine the shrinkage influences on induction of stresses that ultimately sets up transverse cracking; provision is also there to evaluate longitudinal cracking. Another figure is also included here, which denotes a finite element stress contour for normal stresses (acting in x direction) at the midpoint of the concrete deck. The red line in the figure represents various areas of peak stress. In every case mentioned peak areas are located immediate right (or left) of a girder. These are elongated in the longitudinal direction.

This is mainly because of the modeling of diaphragms at the mid pier of the structure. This is most likely caused by the modeling of the concrete diaphragms or pilasters at the center pier in the bridge superstructure. in the finite element model, the diaphragms at the central pier and abutments were modeled with displacement restraint conditions in the transverse (x) direction (Komp 2009). The restraint directions were parallel to the x-axis instead of parallel to the skew. As a result, it appears as the increased stress contours tend to be distorted in a longitudinal direction, as they follow the skewed shape of the bridge. Therefore, the modeling of the diaphragms may cause a slight increase in stress at those locations. The deck deflects with a concave upward shape due to the shrinkage strains (Komp 2009). Therefore, the top of the deck near the exterior edges will be in compression as seen in Figure 4. This also implies that the bottom of the deck will be in tension.

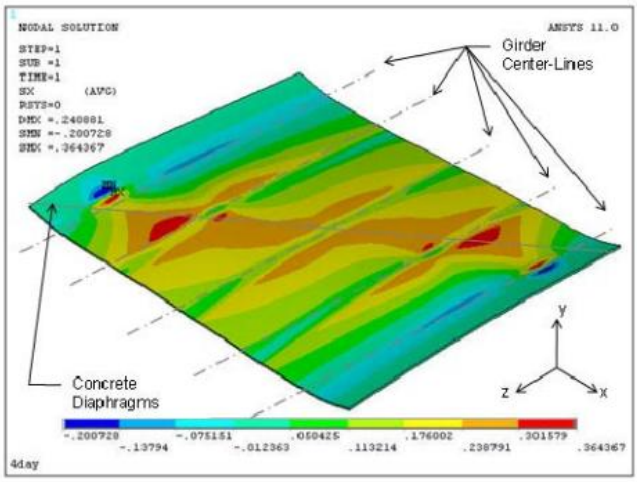

Figure 4: Transverse stress contour on top of deck from Shrinkage Analysis (Komp,2010)

2. “Simulation of the Long-Term Behavior of Precast/Prestressed Concrete Bridges” by Eldhose Stephen (2006)

In this study researcher has tried to simulate phenomenon of creep which is induced because of prestressing force and dead load on the support, differential shrinkage which takes place between deck & support and finally due to cracking induced in the single span concrete deck. The need for a FEM analytical tool was realized very early and after selection from available options, ABAQUS 6.5-1 was chosen for the purpose. The selection was done on the basis of the fact that this software provides the most appropriate combination of tools. The selection was also justified by the ability of the software to effectively use the provisions of the software for modeling a prestressed concrete bridge along with its long term characteristics and time dependent qualities. The fact that numerous facilities are provided in the mentioned software was realized through a proper documentation and number of parametric studies that have been carried out on ABAQUS. A methodological analysis of the records of structures suggested a reason for the gap between observations obtained by experimental methods on real time bridges and analytical approach. The reason was cracking of the concrete deck. The model crafted in ABAQUS here in the study was validated with the help of records of 1993 Federal Highway Administration (FHWA) study of High Performance Concrete (HPC) bridges across the U.S. The bridge passing over the Newfound River in Bristol was used for modeling.

Figure 5: Bridge over Newfound River (Eldhose Stephen 2006)

As mentioned earlier, records and data of FHWA were used in the modeling. The models for geometric and material consideration were also done based on the data from FHWA records.

For the sake of calculating creep and shrinkage, ACI equations were first calibrated to be at the par of already known creep/shrinkage values. After calibration, these equations were used for creep and shrinkage calculations. The study noted that in the event of crack in concrete deck, factors such as Young's Modulus and Yield Stress perform an important role. The values of these variables do affect the timing and location of the cracking. Any inaccuracies in available observations were rounded off by estimation so that model could be made perfectly suitable for the purpose. It can be seen from figure 6 that ABAQUS outcomes matched observations of FHWA studied strains for the bottom flange of support.

An analogy can be made from it which is summarized below. It was noted that the curves obtained even though do not exactly matches with one another, a general trend can be found in terms of some below mentioned features.

1. Increase in strain due to the release of prestress combined with Girder Dead Load.

2. Creep induced progressive increase in strain
3. Spontaneous fall in strain because of deck passive load
4. Steady increase in strain because of a joint effect of creep & differential shrinkage

It was in the conclusion that the curves obtained can be made coincide with one another by changing Modulus of Elasticity and Coefficient of Creep used in the evaluation.

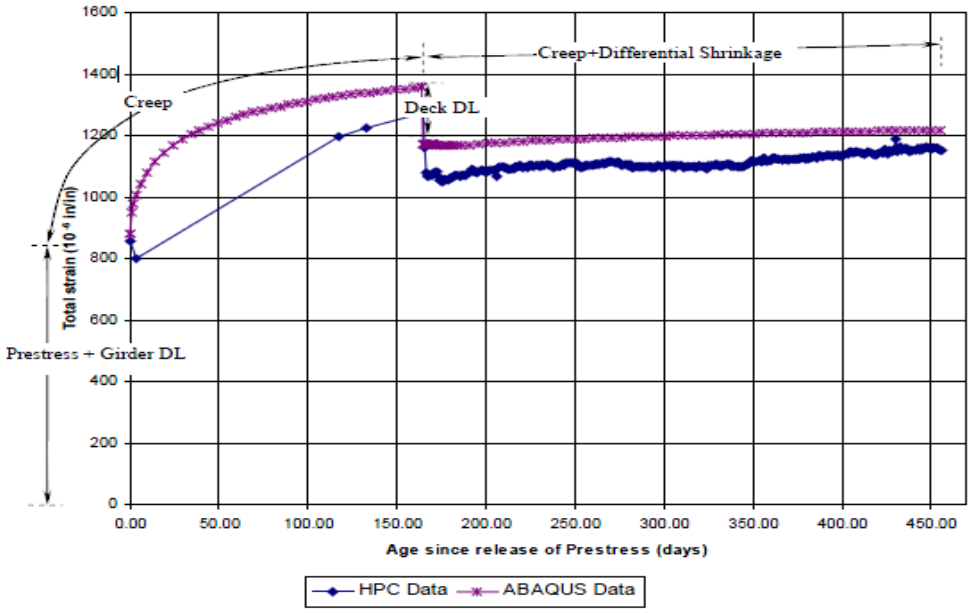

Figure 6: Comparison of Abaqus and FHWA data (Eldhose Stephen 2006)

An analytical model of the chosen bridge deck was made, its analysis was carried out, and the obtained results were compared with the data of field observations. This detailed process was the validation of the bridge deck. The success of the simulation can be identified as it predicted the behavioral conformity of the model. Using girder and reinforcement, the developed abaqus model forecasted constraint to free shrinkage in the concrete deck. This implied the prediction of the cracking occurrence can be done by this model. The ability of the model in achieving so is success of the model. When cracked, deck offers minimal constraint to the supportive girder, which corroborate the unavailability of the variations in strain (or camber) identified in PCA

model. We must note here that the validation done here is of a Simply Supported type of girder. But it is acceptable to apply the obtained conclusions to continuous for Live Load Bridge.

3. “Effect of Intermediate Diaphragms to Prestressed Concrete Bridge Girders in Over-Height Truck Impacts” by Pizhong Qiao, Mijia Yang and David I. McLean (2007).

This study was carried out with the view of developing and validating dynamic numerical finite element models so that it can simulate the prestressed concrete bridge. The study realized the undeniable need of a software package for numerical analysis. The software chosen for this purpose was ABAQUS. This software was chosen over other available options because of its unmatchable ability to conduct preprocessing, solving and post processing evaluations. ABAQUS CAE, which possess a provision for defining material properties, material and geometric modeling, boundary and loading conditions and connections among various elements. ABAQUS provides a tool for solving problem. This tool is split into various options such as static general, static risk for post failure analysis, explicit as well as implicit dynamic analysis. Post processing mentioned above serves the purpose of recovering analysis conclusions in number of ways. It also helps defining stress and/or strain contours. The physical model under the consideration in this study was taken from the ISU study (Abendroth, et al. 2004). The analytical results obtained in this study were matched to experimental observations of the referred study.

In the first step numerical model was developed using FEM. This model was used for impact evaluation of prestressed concrete bridges with Intermediate Diaphragms (IDs) included in it. This model was validated with the experimental observation of the bridge mentioned before. The developed numerical model was utilized to evaluate the effects of IDs on numerous vital

parameters related to performance in the impact event. Various parameters namely ID size and location, girder spacing, frame action, applied load, and analysis are thoroughly studied. The obtained impact resistance then was denoted in form of damaged area and plastically dissipated energy. These are compared with each other.

For this particular model, the type of bridge taken up was of I girder type W42G with deck thickness of 4 inches. The ID/Intermediate Diaphragm was of thickness value 8 inches and extended to the top of the surface of the bottom girder located at the central span. The inclusion of abutments was not considered and boundary condition of simply supported type was applied. The horizontal loads were believed to be active at two points along the lower flange of the support.

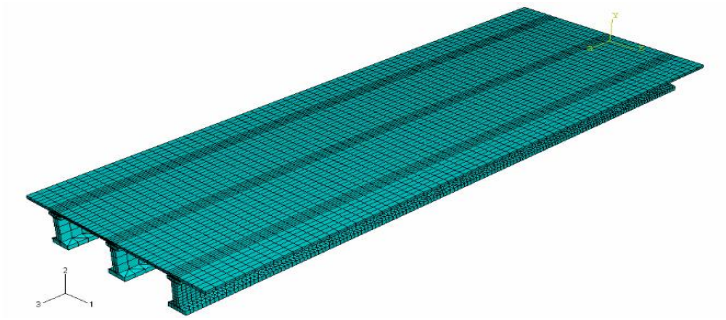

Figure 7: FE mesh of the three girder bridge (McLean, 2007)

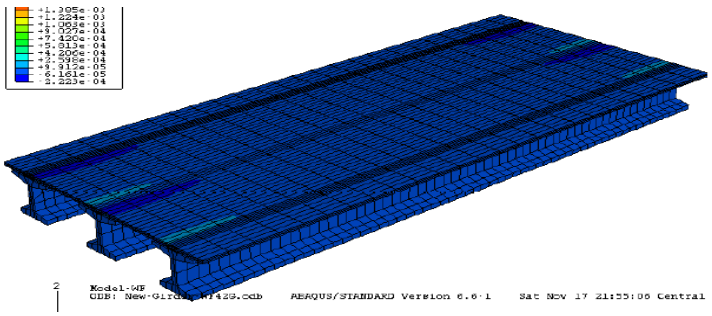

Figure 8: Transverse Strain Distribution (McLean, 2007)

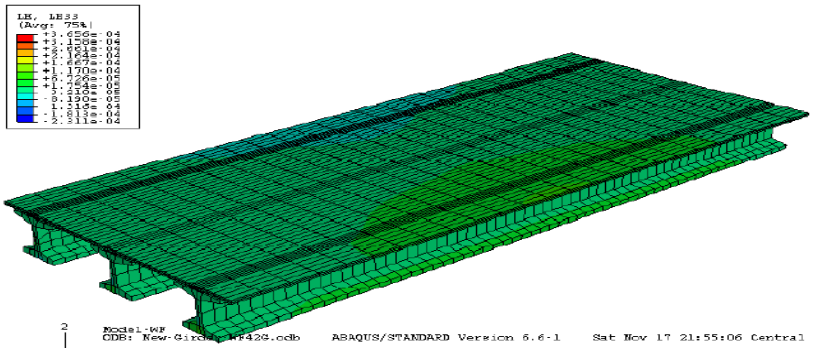

Figure 9: Longitudinal Strain Distribution (McLean, 2007)

The obtained numerical and analytical conclusions coupled with recommendations of ID design and analysis, the bridges are produced to enhance the impact protection of the PC. The researcher from the attained dynamic numerical model and its analysis could find out the bridges performance under impact and also the protection that IDs provide to sustain impact. In the conclusion they have suggested better ways and better methods that can be employed in designing prestressed concrete bridges.

4. “Finite Element Modeling and Analysis of Reinforced-Concrete Bridge Decks” by Michael Biggs (2000).

The study showed that the conventional way of extensive experimentation for gathering observations is very tedious and involves a great deal of time and efforts. The appropriate alternative to the conventional way is to go for Finite Element Analysis for the evaluation. Based on the concept, the analysis was carried out with the help of Finite Element Analysis software ABAQUS. The said package was found to be most proficient and congenial for the given purpose of using it as an alternative to traditional method of analysis. The ABAQUS code was found to be able to accurately represent the nonlinear behavior of concrete. The most striking feature of the

code is to be able to show and use behavior of reinforcing elements independently to the concrete material. The research included making of a 3 Dimensional Finite Element Model for computing and denoting structural behavior of reinforced concrete systems as a reaction to the applied effects. The model successfully forecasted some of the factors such as biaxial strain patterns along elemental thickness, normal girder strains (acting in axial direction-longitudinal) and displacement. The validation process involved the comparison of the obtained numerical analysis results with hand calculations and/or results of laboratory testing.

For certifying the method of numerical analysis it was needed that the simulated model be validated by results of already performed experiment on a real structure. For this purpose, bridge over Willis River along the route 621 was considered. Particularly the composite behavior and typical global reaction of reinforced deck and steel girders were focused. The following stages of the project focused upon the parameterization of the model and its analysis. It has to be noted at this point of review that similar to some other projects related to use of Finite Element Method and software for analysis purpose, this project too considered some assumptions and the study was based on this assumptions. These assumptions were made for simplification of the problem without sacrificing preciseness. Some of the assumptions are mentioned here. The gradient of 1.4% for bridge deck was overlooked, so that the matrix can be set in X-Y plane parallel to axes. The thickness of the deck was averaged to 9.75 for all computations. The steel placement was fixed to remain constant through the deck. One of the major assumptions was not to include 38 mm concrete haunch in the model. The haunch acted as a preventer to shear connecters and as a separator to girder and bottom surface of the deck.

The conjunction between diaphragms and girders was of fixed type and modeled as a node-node conjunction. The multipoint restraints were used to denote the mechanical connections of external elements of the bridge deck in the Finite Element Model.

Following figure represents the model of the entire span, with the deck, parapets, girders, and diaphragms.

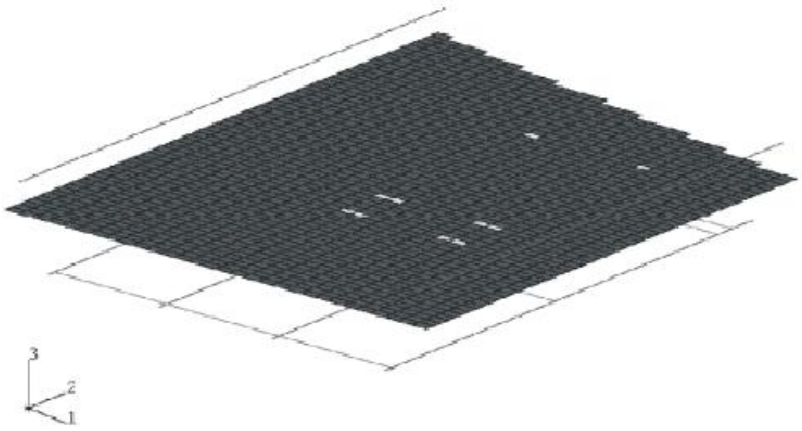

Figure 10: View of Span A and Location of Applied Loads (Biggs, 2000)

Longitudinal as well as transverse stresses induced in the girder and deck are denoted at particular locations. The record under consideration represents the global response of the bridge model. The representation is mainly of compressive and tensile stresses.

The contours of Figures 11 and 12 represent the transverse strain patterns in the concrete deck. In Figure 11, the transverse compressive strain in the upper fiber of the deck is most obvious when considered under the rear-axle load patch. While figure 12 represents the tensile distribution of the deck which can be ascribed to the load.

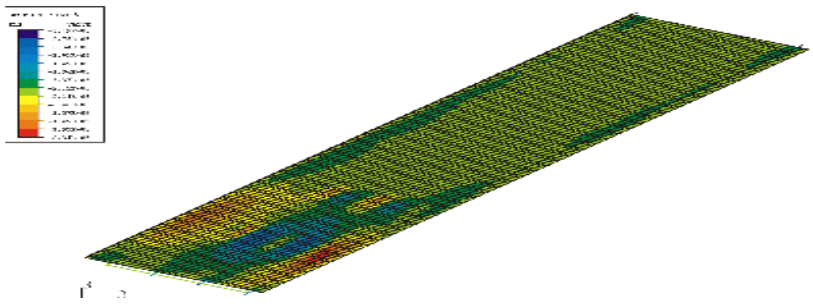

Figure 11: Transverse strain at Top Surface of Deck (Biggs,2000)

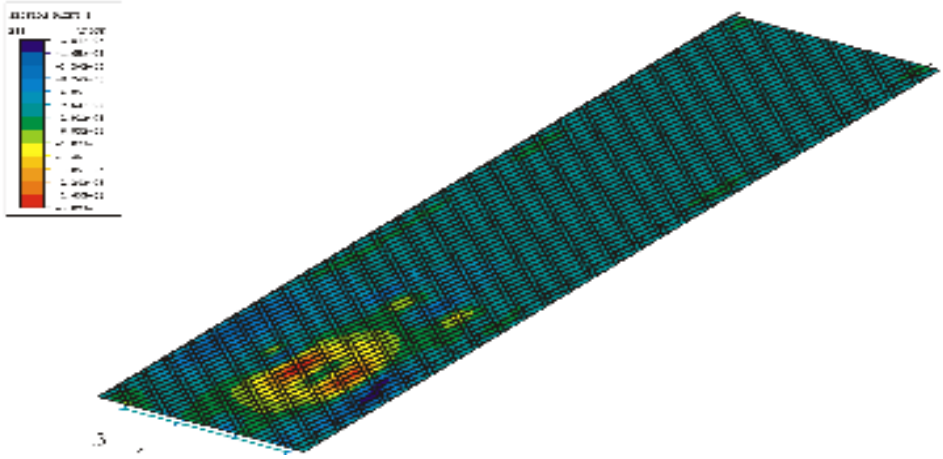

Figure 12: Transeverse strain at Bottom surfsce of deck (Biggs,2000)

The conclusion of the project justifies the ability of ABAQUS to model reinforce concrete precisely thanks to some proficient features involved in it. The preciseness of the finite element model was validated with considering the limitations of FE model to match field observations/ laboratory observations carried under not so ideal conditions were noted. With the successful modeling of the whole bridge corroborated the ability of ABAQUS to evaluate of realistic feasible structures. It also vouched for its capability to accurately forecast deflections, strains and stresses with simplifying complicated problems.

5. “Tool for Analysis of Early Age Transverse Cracking of Composite Bridge Decks” by Levon Minnetyan and Kerop D. Janoyan (2011)

For calculating stresses that are induced in high performance concrete because of the factors and events such as temperature, shrinkage and live/dead loading, analytical as well as numerical methods have been created. The result is establishment of accurate computational methods and related FEM software. The software is nothing but a structural analysis program running with the help of layered finite element model (Layered FEM). This project also took care of heat of hydration involved, which plays a vital role in the development of the cracking in the concrete. The structural analysis code is applied after the layer by layer temperature with respect to time, induced because of heat of hydration is run and computation for the later event has been done. This computational analysis is carried out with the help of thermal FEA. It is very interesting to note that the nodal coordinates that are so vital for carrying thermal finite element analysis, are derived directly from the layer thickness of structural FEM analysis. One of the impressive thing in the development of the model is that the events like autogenous shrinkage, drying shrinkage and stress relaxation or creep are included in the analysis with the help of test data based model. The software was used to calculate time dependent residual stresses for the period of 28 days. After the stipulated time was over, an external load with the help of HS25 vehicle was implied on the model. Again layer by layer analysis of the longitudinal stresses was carried out. This was used to be compared with the modulus of rupture and evaluation of cracking. The most defining part of this project was the fact that for validation purpose, a composite bridge was constructed at the Clarkson University. The thermocouple and strain gage instrumentation were used with the model. Observation of temperatures and strains were taken over the period of again 28 days (as same as period taken in the earlier analysis

approach). After that the specimen was subjected to concentrated loading with the help of Universal Testing Machine. The final stage of the test involved the observation and documentation of cracking phenomenon.

The software results were compared with results obtained in the test. Analysis of the time history temperature contour was carried out with the help of 1-D thermal analysis Finite Element Approach. The coding language used for the purpose was FORTRAN. The program written using FORTRAN utilized the standard 1-D time history FEA as established by Desai (1979).

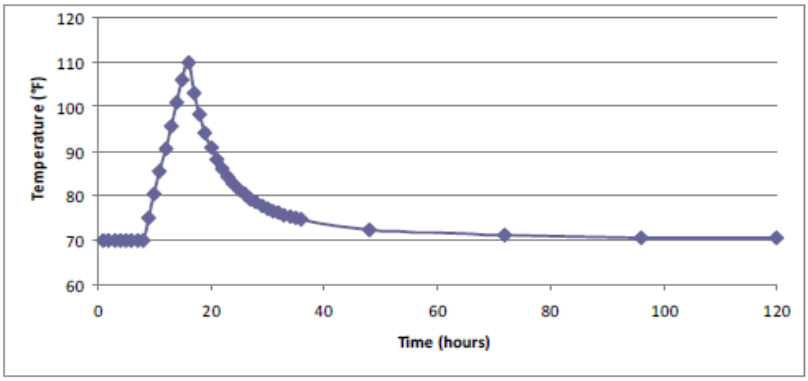

Figure 13: Computed temperature at node 16 corresponding to location of gage T9

(Levon and Kerop, 2011)

The thermal finite element evaluation is intended to interpret data from an existing input file. The file is comprehensive of all the nodes and elemental facts related to the material properties and conditions implied on the deck. The file is particularly crafted to maintain compatibility with the program. A specific file is generated for every single problem. When thermal finite element analysis is compiled and run, a whole new file is generated in the library the same where input file exists. The fact to be noted is that this file carries all the necessary details related to the

analysis. The procedure now can be summarized like this. The first step includes redefining the parameters from the input file as explained earlier. The output file carries analytical results obtained through the program. For every single time step of the input document has corresponding temperatures at nodes. The result of the analysis noted that for all four observations, peak temperature was recorded to be at 16 hours after the pouring concrete. The temperature changes associated with the ambient air was taken care of by the conjunction between steel frame and concrete. This conjunction was intended for acting as insulation only. If this insulation is removed the conclusion of the project will be entirely different. But the noticeable thing is that the program has a provision to allow these modifications.

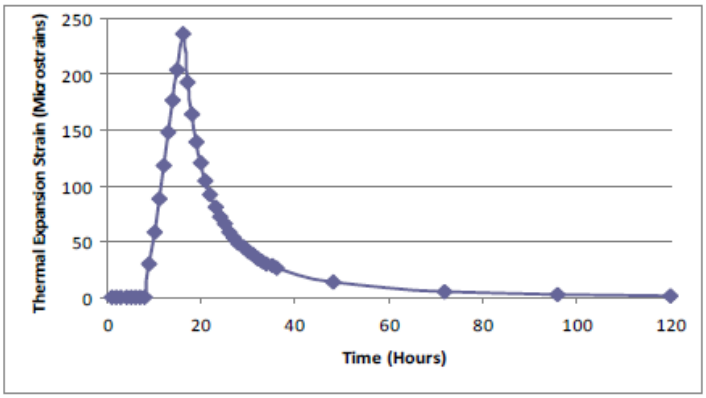

Figure 14: Thermal Expansion Strains during hydration of concrete (Levon and Kerop, 2011)

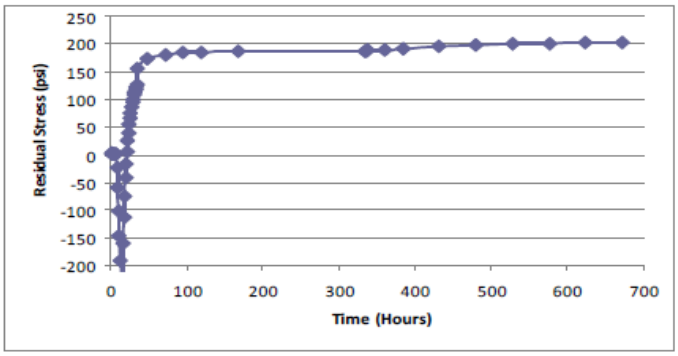

Figure 15: Computed Residual Stresses in concrete at bottom of deck due to Temperature and Shrinkage (Levon and Kerop, 2011)

For computing the time history residual stresses induced because of temperature and shrinkage, a computer program was created and was applied for evaluation. The program also took care of HS25 vehicle loads after 28 days after pouring concrete. It is very obvious that the cracking takes place when the tensile stresses exceed modulus of rupture. Once cracks are formed, the dimensional entities of the crack are worked upon by a finite element model with the boundary conditions. These conditions are obtained from strains which were computed by global structural analysis. The outcome showed that the autogenous and drying shrinkage are main reasons for enhancing tensile stresses in bridge deck. Simultaneously the contribution of hydration heat is not that dominant. In addition to that the temperature effects can be weaken by working on girder temperatures during the initial four days after pouring concrete. The lower flange of the girder is kept at considerably lower temperature, compared to top flange when hydration of concrete would decrease the residual stresses as concrete is cooled down. The bottom half of the flange will be heated up when concrete cools down. This event induces an additional curvature in the deck and it decreases the tension at the surface. The weakening of temperature effects can be done as explained but it is extremely arduous to lower the autogenous and drying shrinkage effects. One of the methods to mitigate the effects of drying shrinkage is to cover the deck with a material having moisture repellent characteristics. A method for autogenous shrinkage is to mix expansive cement in concrete. Bridge when subjected to live loading e.g. load due to vehicles, enhances tension on the deck and this promotes the cracking. Residual stresses in the concrete deck have been found to be proportional to depth of the girder. This is due to the fact that bigger the girder the more constraint is acting on the shrinkage of the concrete. It is worthy to note that the stresses due to live loading are inversely proportional to the depth of the girder. Optimization among the all factors needs to be achieved so that cracking propensity is reduced. The computational

simulation with the aim of optimization concludes that increasing girder depth results in betterment in overall cracking propensity.

1.4 Objective Of Research

Due to many variables responsible directly or indirectly for shrinkage which ultimately results in cracking, it is very difficult to study the overall effect of these variegated factors taken in the consideration at a time. This thesis aims to confluence as many such aspects as possible in a single plane of consideration with the help of Finite Element Methods and FE software primarily ABAQUS.

The goal of this research is to study the shrinkage effects and to incorporate the shrinkage effects into Finite Element Modeling. Here the study is constrained to Prestressed Concrete Bridge. The parametric study is carried out to analyze shrinkage effects in prestressed concrete bridge.

CHAPTER 2

Shrinkage Models

2.1 Shrinkage

It is natural propensity of any material to react to any action imposed upon it or any event or process occurs and the material is involved in it. Similarly in the case of Concrete; it is concrete's inclination to undergo volume changes due to one or other event or process. It is a universal fact that whenever any constraint or restriction is applied to naturally occurring phenomenon, some kind of disturbances induces. For concrete deck, if there is no restraint present, the changes in the material properties (our case focuses on volumetric changes) takes place without causing any stresses. The concrete mass merely changes in volume in the absence of any binding or preventive force. It should be noted that the strains do get produced but no stresses are generated. In this case no cracks are formed. But in actual field application the above case is an ideal one and does not hold true. This is because elementary members such as foundations, reinforcement and connecting members all offer some kind of resistance/ restraint. For evaluating volume alterations, the causes of these changes have to be analyzed properly.

Usually the volume changes are denoted linearly when it is related to concrete. The reason for it is the fact that most concrete constituents are very long in a particular direction compared to their magnitude in other two dimensions. The contraction of the volume is mainly ascribed to moisture and temperature effects. The changes explained here have been given a general term "Shrinkage".

Shrinkage can thus be defined as Volume alterations of the concrete that induce due to inherent properties of the material. The shrinkage phenomenon is inevitable in concrete, but the magnitude and techniques employed to reduce it or even to utilize it are of prime importance. In general term shrinkage is used to explain various aspects of volume changes in concrete due to loss of moisture at different stages due to different reasons. Thus Technically Shrinkage of concrete is the time-dependent strain measured in an unloaded and unrestrained specimen at constant temperature. According to the timing and reasons of the induced shrinkage, shrinkage has been classified in four sub categories namely: Plastic Shrinkage, Thermal Shrinkage, Autogenous Shrinkage and Drying Shrinkage.

Shrinkage is one of the most powerful roots of cracking in bridge decks (Krauss and Rogalla, 1996; Phillips et al., 1997). Studies have shown that restrained shrinkage alone can induce tensile stresses strong enough to produce cracks on the deck. If the deck shrinkage is 0.5milistrain, the induced tensile stresses can be as bigger than 1000 psi, with material properties and geometric constraints playing their parts (Krauss and Rogalla, 1996).

2.2 Types of Shrinkage

Concrete shrinkage has become one of the most studied and discussed areas when it comes to durability of a structure. Shrinkage is believed to be a main culprit responsible for cracking, which eventually decreases the concrete life significantly. Thus shrinkage as mentioned in the first statement impacts durability of the structure in a great measure. The most common root cause in cracking- shrinkage is classified in four types according to its origin and its nature. The four categories are listed and explained below.

- Plastic Shrinkage
- Thermal Shrinkage
- Autogenous Shrinkage
- Drying Shrinkage

Shrinkage starts off instantly after the pouring of fresh concrete. The changes in volume can continue for coming years after curing is done. The type and rate of shrinkage is often determined by the factors such as Cement properties, type and gradation of aggregates, rate of drying. The section below discusses the types of shrinkage in detail. It should be noted that shrinkage has not been fully evaluated in a perfect manner. Specific tests can help distinguish between various types of shrinkage, yet the actual mechanisms through which these types takes place are subjects of discussion.

2.2.1 Plastic Shrinkage

Plastic shrinkage is also called early age shrinkage; this is due to the timing of the occurrence of it. Issa (1999) noted plastic shrinkage as the most influential root of bridge deck cracking. This takes place at the surface of the fresh concrete. After the concrete has been poured, excess water travels to the surface of the poured concrete. This phenomenon is bleeding of water towards surface. There is a simultaneous process of evaporation of water from the surface. When the rate of evaporation of water from the surface is greater than the rate of bleeding towards surface, a differential current takes place which yields shrinkage known as plastic shrinkage or early age shrinkage. At this point of time independent water layer of existing in the concrete falls within the concrete which induces menisci between particles. These menisci impart tensile pressure on the particles due to surface tension. This pressure acting on a low strength concrete (due to drying of top surface) induce cracking in the concrete (Mindess and

Young, 1981; Cheng and Johnston, 1985; Holt, 2001; Brown et al., 2001). As these cracks are originated at the surface of the concrete they are limited to near depth from the top surface. Yet they are strong and deep enough to promote chloride and water penetration and also stress concentration for subsequent years of service of the structure. It should be noted that this type of cracks are never longer than 2-3 feet or 2-3 inches in depth (Xi et al., 2003, Krauss and Rogalla, 1996). The configuration of plastic shrinkage cracks are of "Turkey Track" type. The previous studies and results of experimental tests show that the bleeding rate is lower in the case of HPC compared to normal concrete. This means this type of concrete is more prone to plastic shrinkage. If evaporation process is restraint or controlled, control over this type of cracking can be achieved. Fogging, windbreaks, shading, plastic sheet covers, or wet burlap are most commonly used as a guard against plastic shrinkage.

2.2.2 Thermal Shrinkage

Most of the natural chemical processes involve transactions of the heat. In case of analyzing shrinkage, heat is extracted in the hydration process in the concrete. The hydration of the cement mixture takes place after pouring concrete and this produces the heat, often named as heat of hydration. This process causes concrete to expand/prolong during initial curing period. As curing process proceeds further, the temperature gradually gets decreased and the concrete faces contraction in the volume as a natural response to the action caused in the first stage. This spontaneous volumetric contraction (in other words thermal contraction) induces cracking in the concrete. This type of cracking due to very fact of its origination is called thermal cracking. And the process of shrinking of concrete volume is known as Thermal Shrinkage. In other words the thermal shrinkage in the concrete takes place due to inability of the concrete to remove heat fast enough and/or effectively enough. If a structure is thinner the heat transfer area is

more and hence heat extraction occurs at very high rate. This means this kind of structures are less prone to thermal shrinkage and hence to thermal shrinkage cracking. A bridge deck is considered to be a slender structure on larger context of the definition of structures and therefore the thermal shrinkage and thermal shrinkage cracking is believed to be negligible in this case.

2.2.3 Autogenous Shrinkage

Autogenous Shrinkage in simple words has been defined as the change/ alteration in volume induced due to hydration of the cement. The process of autogenous shrinkage is very simple for explaining purpose but when it is needed to be incorporated in computations and numerical analysis it becomes extremely complex. The actual phenomenon of autogenous shrinkage I concrete can be explained as follow. After the concrete has been poured, curing takes place. Curing process involves watering cement. This is sophisticatedly called hydration of cement. It is very obvious that the hydration process uses water. When there is no or insufficient external source of water is available, cement turns toward internal water masses. These internal masses include pores and voids of the concrete. Thus the binding water mass from the concrete is taken up by cement for hydration. Continuous consumption of this internal water by cement in hydration process desiccates the gorges, voids and pores. This eventually causes concrete volume to shrink. So this continuous consumption of water in hydration and continuous desiccation of water from internal water masses causes shrinkage in concrete volume. This is known as Autogenous Shrinkage. The main reason in a nut shell for autogenous shrinkage can be identified as Self Desiccation.

The above explanation of the event shows that this process occurs only if there is insufficient water is available. The simple logic that can be concluded is, if sufficient amount of water is provided the chances of this type of self-desiccation is nullified. Thus, more the water available lesser are the chances of autogenous shrinkage. To avoid shrinkage of this kind, practically large amount of water is made available so that even after the hydration process excess of water is available. It is also worthwhile to note at this point of discussion that the concrete with higher water to cement ratio suffer less problem of autogenous shrinkage (Vinod Rajyogan). This is obvious as more water content takes care of the need in hydration process. Inversely the concrete with low water to concrete ratio are highly susceptible to autogenous shrinkage. An example of this kind of concrete is HPC.

Careful evaluation of this phenomenon shows that constant and rapid drawing of water from internal water sources by hydration process generates fine capillaries. The surface tension of these capillaries imparts tensile stresses and which in turn induce cracking. A note should be taken that autogenous shrinkage is completely from the conventional drying shrinkage. The conventional drying process occurs only after curing is completely carried out. While autogenous shrinkage happens once any transaction of moisture between surface and ambience is ceased.

The development of the internal capillaries which ultimately governs the shrinkage process, is dependent of mainly three factors namely concrete's chemical shrinkage, amount of bleeding and time of hardening (Erika Holt, 2001). As this kind of shrinkage is mere result of chemical composition and structural reactions of compositions, it is often known as "Chemical Shrinkage". For nature of the phenomenon it is also called "Self Desiccating Shrinkage". The role

of autogenous shrinkage was often viewed as “not so important” in previous times considering dominating role of Drying Shrinkage. But as in recent times more and more usage of high performance concrete (low water to cement ratio) and specialized concrete have forced designers and engineers to give proper attention to this shrinkage. Minimum seven days of curing is believed to be capable of eradicate the problem of autogenous shrinkage. Nowadays usage of specialized admixtures has also been found to be extremely capable method.

2.2.4 Drying Shrinkage

The drying shrinkage has been identified as one of the most damaging shrinkage occurring in concrete mix. It is often labeled as the most harmful characteristics of Portland cement composites (Zhang and Li, 2001). The drying shrinkage is outcome of volume alterations in concrete as a result of evaporation process. The distinction of this type of shrinkage is that, this process continues for long period of time after the concrete has been placed. The chemistry of the drying shrinkage is similar to plastic shrinkage with the only difference that the former one takes place once concrete has been hardened. When the water is driven away from concrete to ambience, the tensile stresses are induced due to drying up of pores. With continuation of this transfer of water, equilibrium is attained and the moisture movement is now totally governed by environmental conditions. This implies if conditions are watery or wet concrete will swell; and if it is arid the concrete will shrink (Mindess and Young, 1981). At this point if there is no constraint or hindrance on shrinking volume no strain will be converted into stresses. But in practical cases, all structures impart constraint and hence stresses are induced. Shear connectors, foundations, supportive elements etc. act as sources of restraint. Structures with lower surface to volume ratios are less prone to drying shrinkage. Inversely bridge decks having low surface area to volume ratios are more prone to drying shrinkage. In this type of shrinkage,

water to cement ratio too plays a vital role. The lower the water to cement ratio, possibility of drying shrinkage is lesser. Moreover aggregate properties too play an important role. Harder aggregates such as quartz, granite, feldspar, limestone and dolomite have been found to counteract the effects of drying shrinkage due to their high resistance to compression (ACI Committee 224). Various methods of wet curing will postpone or delay drying shrinkage till completion of curing.

2.3 Shrinkage Prediction Equation

There has been recorded a significant progress in the field of creep and shrinkage. The last two decades have recorded a considerable understanding of creep and shrinkage phenomenon. The concrete creep which is also called as stress relaxation process and concrete shrinkage have been thoroughly studied and grasped through various studies and projects over the years. This grasping has helped attain proper understanding of the physical mechanisms involved in creep and shrinkage processes. The outcome is successful development of the mathematical models incorporating these events.

During literature review of this research, following three shrinkage models have been studied and referred to largely. These models are as discussed below.

Three shrinkage prediction models mentioned above are namely:

1. ACI – 209 Code Model (ACI 209)

2. Bazant Model B3 (Bazant)

3. Comite Euro-International Du Beton Model Code 1990 (CEB90)

1. ACI-209 Code Model (ACI 209)

The general equation for predicting shrinkage of concrete is given by following equation:

$$(\varepsilon_{sh})_t = \frac{t^{\alpha}}{f + t^{\alpha}} \cdot (\varepsilon_{sh})_u$$

Where $(\varepsilon_{sh})_t$ is the time dependent shrinkage strain, $(\varepsilon_{sh})_u$ is the ultimate shrinkage strain, t is

The time after loading, f is in days, and α depends on size and shape of the specimen. For shrinkage after age 7 days for moist cured concrete, ACI recommends a value of 35 for f. The previous equation then becomes:

$$(\varepsilon_{sh})_t = \frac{t^{\alpha}}{35 + t^{\alpha}} \cdot (\varepsilon_{sh})_u$$

In the case of absent specific shrinkage data for local aggregates and conditions, ACI recommends the following average value:

$(\varepsilon_{sh})_u = 780\,\gamma_{sh} \times 10^{-6}$ in/in (m/m)

Where, γ_{sh} is the product of the ultimate shrinkage strain under standard conditions by applicable factors. These factors include initial moist curing, ambient relative humidity, and average thickness of member or volume –surface ratio, temperature, and concrete composition.

2. Bazant Model B3 (Bazant)

The shrinkage prediction equation by Bazant is given below.

Time-dependence of ultimate shrinkage:

$\epsilon_{sh\infty} = \epsilon_{s\infty} \frac{E(607)}{E(t0+\tau sh)}$

$E(t) = E(28)\left(\frac{t}{4+0.85t}\right)^{1/2}$

Where, $\epsilon_{s\infty}$ is a constant.

$\epsilon_{s\infty} = -\alpha 1\alpha 2\ [26w^{2.1} f_c^{-0.28} + 270]$ (in 10^{-6}) inch-pound system

$\epsilon_{s\infty} = -\alpha 1\alpha 2\ [1.9 \times 10^{-2} w^{2.1} f_c^{-0.28} + 270]$ (in 10^{-6}) SI

Where,

α1 = 1.0 for type I cement;

0.85 for type II cement;

1.1 for type III cement.

and

α2 = 0.75 for steam-curing;

1.2 for sealed or normal curing in air with initial protection against drying;

1.0 for curing in water or at 100% relative humidity.

3. Comite Euro-International Du Beton Model Code 1990 (CEB90)

In this project the researcher has adopted CEB-FIP model for predicting shrinkage induced strain. The following model which was developed by CEB-FIP was used in the project for predicting the strains.

$$\varepsilon_{cr}(t, t_0) = \frac{\sigma c(t_0)}{E_{ci}}\ \phi_{28}(t, t_0)$$

Where $\varepsilon cr(t,t0)$the creep strain at time t is, $\sigma c(t0)$ is the applied stress, Eci is the modulus of elasticity at the age of 28 days, and $\phi 28(t,t0)$ is the creep coefficient

Where in the determination of modulus of elasticity can be done by the following equation.

$$E_{ci} = \alpha_E \ 10^4 \left(\frac{f_{ck} + \Delta f}{f_{cm0}}\right)^{\frac{1}{3}}$$

Where fck the characteristic strength of concrete in MPa is, Δf is equal to 8 MPa, $fcmo$ is equal to 10 MPa, and αE is equal to 2.15x104 MPa.

The creep coefficient $\phi 28(t,t0)$ can be computed by the following equation.

$$\phi_{28}\ (t,t_0) = \phi_0 \ \cdot \ \beta_c\ (t - t_0)$$

Where $\phi 0$ is the notational creep coefficient, βc is the coefficient to describe the development of creep with time after loading, $t$is the age of concrete in days, $t0$ is the age of concrete at the time of loading in days.

The notational creep coefficient $\phi 0$ can be computed by the following equations:

$$\phi_0 = \phi_{RH} \ \cdot \beta(f_{cm}) \ \cdot \ \beta(t_0)$$

$$\phi_{RH} = 1 + \frac{1 - \frac{RH}{RH}}{0.46 \ \cdot \left(\frac{h}{h_0}\right)^{\frac{1}{3}}}$$

$$\beta(f_{cm}) = \frac{5.3}{\sqrt[2]{\frac{f_{cm}}{f_{cm1}}}}$$

$$\beta(t_0) = \frac{1}{0.1 + \left(\frac{t_0}{t_1}\right)^{0.2}}$$

$$\beta(t - t_0) = \left[\frac{\left(\frac{t - t_0}{t_1}\right)}{\beta_H + \left(\frac{t - t_0}{t_1}\right)}\right]^{0.3}$$

$$\beta_H = 150 \cdot \left[1 + \left(1.2 \cdot \frac{RH}{RH0}\right)^{18}\right] \cdot \frac{h}{h_0} + 250 \leq 1500$$

Where $f_{cm} = f_{ck} + \Delta f$, $h = \frac{2Ac}{u}$ is the notational size of the member in mm, Ac is the cross sectional area in mm2, u is the perimeter of the member exposed to the atmosphere in mm, h_0 is equal to 100 mm, RH is the relative humidity of the ambient environment expressed in %, $R\text{H}_0$ is equal to 100%, and t_1 is 1 day.

2.4 Incorporating Shrinkage into FE

The analysis of occurrence and related events and causes associated with the cracking phenomenon has been evaluated precisely thanks to the technological betterment and constant evolution of the analysis software and related tools and provisions within. The most striking thing to be noted is that ability of the finite element software packages/ tools that have enabled incorporating characteristics driven phenomenon. This has enabled the forecasting behavior with extreme correctness. Even among the software packages available for analysis, ABAQUS has stood out unmatchable for serving the desired purpose. This is largely due to distinct capability of the software to incorporate factors and variables that largely or sometimes even solely depends upon the materialistic characteristics and properties, the given set of boundary as well as initial conditions and bonding behavior. In addition to the aforementioned qualities of the application software, it should be noted that the preciseness do depend upon the interpretation of the modeling constituents, program and restraining conditions applied. The

various studies related to analysis of such time dependent phenomenon shows that ANSYS too performs the role very efficaciously and has been found very congenial for this type of problems.

From the number of available options of models for finding shrinkage, in this research we have used ACI 209 Shrinkage Prediction Equation for prestressed concrete bridges. The selection of adopting any prediction model is done based on appropriateness to the problem statement. As mentioned, for this problem ACI 209 shrinkage prediction equation was implied. To incorporate shrinkage into FE analysis Abaqus is used with User Subroutines. It is to be noted that Abaqus do not provide tools and features in built that can take care of estimating time dependent phenomenon or events such as creep and/or shrinkage. On the contrary it is extremely important to utilize the credibility of the software in any way to correctly incorporate aforementioned characteristics for precise evaluation of the same. This is done in the Abaqus with the help of user subroutines. The inclusion of these events in the Abaqus is done by introducing shrinkage and creep phenomenon in 'user specified mode' with the help of a user subroutine written in FORTRAN language. These means a separate programming code written in FORTRAN language will help incorporate shrinkage and creep in Abaqus.

As mentioned earlier as well, the time dependency of the events of creep and shrinkage have to be addressed correctly to ensure the success of the analysis. For software to find out creep and shrinkage with help of user subroutines, package needs definition of material properties of deck and girder concrete. Looking at the equation of the creep and shrinkage, it can be inferred that the creep depends upon elastic strain. On the other hand shrinkage depends upon thermal strain. Abaqus software defines the total strain say E as overall effect of the various constituent

strains such as Elastic Strain (EE), Inelastic Strain (IE) and the thermal strain (THE). Where in the inelastic strain IE is total effect of Plastic Stain (PE) and the Creep Strain (CE). It is to be noted here that the Modulus of Elasticity of deck and girder concrete is age dependent, meaning over the period of time or over the age of the concrete the Modulus of Elasticity suffer alteration. This means to simulate analysis in Abaqus and ultimately find out effects of creep and shrinkage in the bridge, it is absolutely necessary to call instantaneous elastic strain EE & thermal strain THE at each increment and then put it into equation as a thermal strain. This purpose can be achieved using USDFLD and UEXPAN subroutines.

1. User Subroutine USDFLD

USDFLD subroutine is used to obtain precise instantaneous values of elastic strain and thermal strain. The general procedure that was followed here is explained below. For accessing material point data and to define variable GETVRM and STATEV commands can be used respectively in USDFLD. Strain in axial direction is introduced using ARRAY () command. Two variables are defined STATEV (1) and STATEV (3). STATEV (3) contains values of instantaneous elastic strain EE, while values of thermal strain THE is taken care of by STATEV (1). The most striking feature of USDFLD is that it allows defining field variables at a material point as the functions of time. This means a time dependent phenomenon can be expressed as a function of time using this subroutines. In case of a bride model the modulus of elasticity of deck and girder concrete is age dependent which means it varies with time. Hence the modulus of elasticity is defined as a function of field variable in input file. Therefore inclusion of young's modulus in the analysis is done using "IF . . ELSE" loop in USDFLD subroutines. Thus, this subroutine ensures the dependency of the elasticity modulus on time and implements changes accordingly to extract

precise values of instantaneous values of strain which can be used in creep and shrinkage equation recommended by ACI 209 (1992).

2. User Subroutine UEXPAN

For the purpose of this analysis the thermal strain is calculated as a function of the instantaneous strain and time right from the time of loading, using the ACI 209 (1992) equations. In this subroutines incremental stain is used. The subroutine calculates and returns the increment in thermal strain. To take care of which, the equation is modified as incremental strain to find out shrinkage and creep as per ACI209 eqn. UEXPAN can be used to define incremental thermal strains as functions of state variables.

For calculating creep in girder EXPAN (3) and STATEV (3) are used which provide instantaneous value of EE. To apply incremental creep in the girder elements 'IF. .THEN' loop is used that corresponds to girder material and time. The equation used to find creep as incremental thermal strain is,

EXPAN(3)=0.94656*EE*(Tn^0.6/(10+Tn^0.6)-T(n-1)^0.6/(10+T(n-1)^0.6))

For calculating shrinkage in deck EXPAN (1) is used as function of STATEV (1) which contains value of thermal strain THE. Shrinkage strains cause significant long-term effects as far as the deck is concerned. 'IF. .THEN' loop is used with deck material name and time to find out shrinkage in deck. This is similar to what we do for calculating creep. The equation used to find shrinkage as incremental thermal strain is,

EXPAN (1) = -T/ (35+T)*8E-4+TL/ (35+TL)*8E-4

Thus the above two paragraphs with two equations explains how UEXPAN Returns the values for creep and shrinkage increments, calculated using equations as per the recommendations of ACI 209 (1992).

CHAPTER 3

Finite Element Model Validation

3.1 Design of Bridge (P/C) and Data Base

3.1.1 Design of Bridge (P/C)

As discussed in earlier chapters, ABAQUS was identified as the most appropriate analysis tool for carrying this research on prestressed concrete bridges to evaluate time dependent effects such as shrinkage. Using this software prestressed concrete bridges were modeled. The tool ABAQUS has numerous application in the engineering world but it has been proved to be the most useful when it comes to analysis of time dependent properties of a structure. The tool has been widely used in this field.

The determination of the shrinkage in prestressed concrete bridge was done as mentioned by developing different prestressed concrete bridge models. More specifically, user subroutines were applied to find out shrinkage effects in concrete bridge. The method and procedure that was followed to design bridges is represented in detail by an example of design of a bridge in the appendix A.

Bridge 1

Geometric Properties:

1. Girders
    - AASHTO TYPE Ⅱ
    - Span - 62.833
2. Prestressing Strands

- Grade - 270
- Diameter - 0.5 in
- Initial stress in Prestressing steel - 202.5 ksi

3. Deck

- Width - 282 in
- Thickness - 8 in

Material Properties:

The material of constituent elements such as girder concrete, deck concrete material, Rebar Steel and the prestressing strand steel are presented here in this segment. .

1. Girder Concrete
    - Unit Weight - 0.15 k/ft3
    - Compressive strength - 7 ksi
    - Modulus of Elasticity - 4820.754 ksi
2. Deck Concrete
    - Unit Weight - 0.15 k/ft3
    - Compressive Strength - 4 ksi
    - Modulus of elasticity - 3644.149 ksi
3. Steel & Rebar
    - Modulus of Elasticity - 29000 ksi

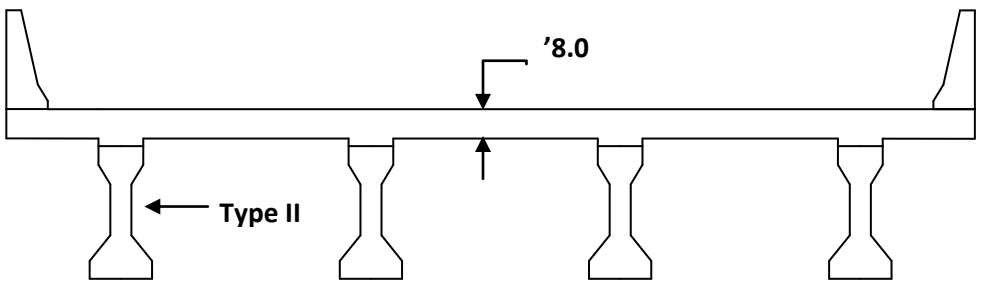

Figure 16: Girder of Bridge 1

Table 1: Strand Patterns of Bridge 1

Bridge 1			
Layer	Number of Strands	Total Cross Sectional Area (in^2)	Distance from top of the girder (in)
1	6	0.918	33
2	8	1.224	31
3	6	0.918	29
4	4	0.612	27
5	2	0.306	15
6	2	0.306	13

3.1.2 Database for Parametric Study

One of the main objectives of this research was to be able to carry an accurate parametric study of various factors of bridge that affects the behavior of it. More specifically, in this research factors such as Bridge Length, Girder Spacing, Deck Thickness, Type of Section and Compressive Strength of Girder f'c, girder restrained condition, these factors were chosen as governing

variables and a parametric study of the bridge with effects of these parameters on shrinkage was carried out. In this section, a segmentation according to the parameter is done and accordingly group of bridges are categorized; meaning a number of bridges are taken from NCHRP under a category with all the parameters except the one with respect to which the study is carried keeping constant; e.g. parametric study with respect to length is done with the bridges with different lengths but all other parameters being same. This procedure is carried over for all the parameters as mentioned above.

The following section contains five groups each for specific parameters. For the bridges chosen for parametric study have following constant entities.

- Compressive Strength of the Deck f'c = 4 ksi
- Initial Stress in Prestressing Steel = 202.5 ksi

The variables that do change with respect to selection of parameters are described categorically in below segment.

1. Parametric Study with respect to Length

(All Bridges are of Section Type = AASHTO III)

Table 2: Bridges for Parametric Study with respect to Length

Span Length (ft)	Spacing of Girder (ft)	Deck Thickness(in)	Compressive Strength of Girder f'c (ksi)	Aps (in^2)	Eccentricity at Midspan (in)
80	6	8	8	3.366	17.00
100	6	8	8	5.814	15.43
60	10	8	8	3.06	15.87
80	10	8	8	4.896	16.02

2. Parametric Study with respect to Girder Spacing

(All Bridges are of Section Type = AASHTO III)

Table 3: Bridges for Parametric Study with respect to Girder Spacing

Spacing of Girder (ft)	Span Length (ft)	Deck Thickness(in)	Compressive Strength of Girder f'c (ksi)	Aps (in^2)	Eccentricity at Midspan (in)
6	80	8	8	3.366	17.00
8	80	8	8	4.284	16.41
10	80	8	8	4.896	16.02

3. Parametric Study with respect to Deck Thickness

(All Bridges are of Section Type = AASHTO IV)

Table 4: Bridges for Parametric Study with respect to Deck Thickness

Deck Thickness(in)	Span Length (ft)	Spacing of Girder (ft)	Compressive Strength of Girder f'c (ksi)	Aps (in^2)	Eccentricity at Midspan (in)
6	100	8	8	5.814	20.52
8	100	8	8	5.814	20.52
10	100	8	8	5.814	20.52

4. Parametric Study with respect to Compressive strength of the Girder f’c

(All Bridges are of Section Type = AASHTO III)

Table 5: Bridges for Parametric Study with respect to Compressive strength of the Girder f’c

Compressive Strength of Girder f'c	Span Length (ft)	Spacing of Girder (ft)	Deck Thickness (in)	Aps (in^2)	Eccentricity at Midspan (in)
6	60	10	8	2.754	16.71
8	60	10	8	3.06	15.87
10	60	10	8	2.448	16.77

5. Parametric Study with respect to Restrained Conditions

(All Bridges are of Section Type = AASHTO III)

Table 6: Bridges for Parametric Study with respect to restrained condition

Span Length (ft)	Spacing of Girder (ft)	Deck Thickness(in)	Compressive Strength of Girder f'c (ksi)	Aps (in^2)	Eccentricity at Midspan (in)	Restrained Condition
80	6	8	8	3.366	17.00	Pinned-Roller
80	6	8	8	3.366	17.00	Pinned- Pinned
80	6	8	8	3.366	17.00	Fixed-Fixed

3.2 Model Description

3.2.1 Introduction

This study utilized and banked upon the general purpose ABAQUS software. This package permits for designating material behavior & characteristics, applicable set of boundary conditions, reinforcement and behaviors of the conjunctions. The grasping and interpreting ability of the user affect the success of the model greatly and key aspects to be taken care of in this matter are model constituents/elements and restrictive conditions. The preciseness of the

model largely depends upon above mentioned two variables. The subsequent segment here explains each model element used as well as the constraint/release conditions applied. Inclusion of the mandatory geometric and/or behavioral modeling features; creep as well as shrinkage capabilities were written in Abaqus Input file. The object oriented approach was carried while defining problem statement in the ABAQUS. This includes definition of each and every single constituent of the model separately maintaining the compatibility with one another. The modeling process itself has to be iterated many a times to successfully attain an objective for simulating specific properties accurately. As ABAQUS cannot alter any non-conforming units later, the system of units need a serious attention while modeling itself. This implies conformity has to be ensured for defining geometric, material and loading conditions/properties.

3.2.2 Geometric Modeling

The definition of geometric properties of the structure was carried out in this section of modeling. The structure of the bridge can be modeled using nodes, elements and sections provided by Abaqus.

- Elements

The ABAQUS program library itself provides numerous options for selection of geometric elements. Out of which for this project, Beam and Shell elements have been identified as the most appropriate and dependable for bridge related problems.

1. Beam Element

Due to its one-dimensional characteristics, definition of stringers and girders can be modeled with the help of Beam Element. Two node beam element is used to model girder. It should be noted here that the segment generally won't deform out of plane. This fact/ condition can be considered a constraint while defining problem statement. This restriction ensures that the

plane section will remain the plane section until whole analysis is done. Figure 17 below depicts the beam element with various integration localities. It is observed that the more minutely modeling is done the more preciseness is achieved. This means the accuracy of the outcomes depends upon the degree of discretization. But the problem a user encounters during working with highly discretized bridge is, slow processing of the program.

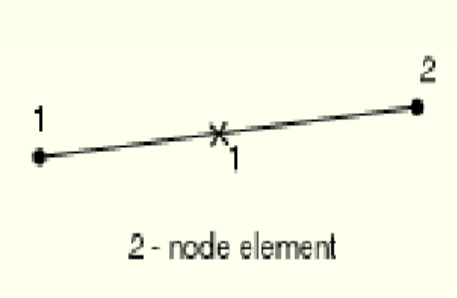

Figure 17: Integration points of two-node linear beam B31

2. Shell Element

For defining models for concrete bridge decks in FE package, a shell element has been used very commonly due to less magnitude of the dimensions in terms of thickness of the slabs in comparison to its other dimensions. The inbuilt library resource for the shell element is very rich. It has been found that the majority of it is of four node type of shell elements. The element is of a completely integrated, general purpose type with finite-membrane-strain shell element that allows in-plane bending able to permit planar bending (in plane bending). In addition to this, it also allows deflection/deformation in transverse direction. It should be noted that this element is considered to be a thick shell theory. This is very certain as this hypothesis banks upon the condition of homogeneous isotropic materials. Thus implementing it for thick-shelled, laminated anisotropic materials, such as the steel reinforced concrete bridge deck will not yield

proper results. The four-node shell element has six degrees of freedom at each node and four integration points for each element. Figure 18 illustrates the integration point and nodes used by the four-node shell elements.

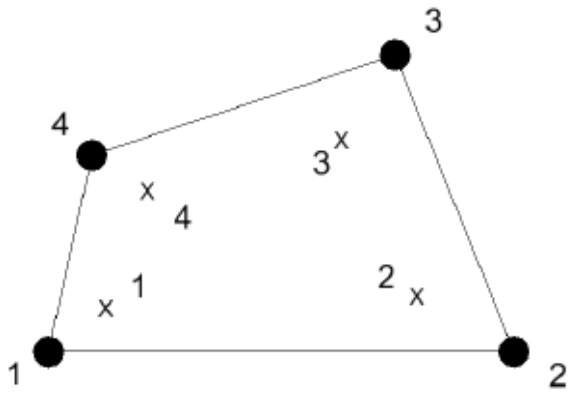

Figure 18: Integration points of a four-node shell element (Abaqus)

- Fineness of the Model

Model will require fine tuning to get accurate results. The fine tuning of the model can be achieved by giving appropriate element size. Although increasing the fineness of the finite element of any model ensures greater accuracy, it also causes a correspondent increase in the size of the stiffness matrices involved and therefore longer analysis times

- **Sections**

It is extremely important and inevitable to incorporate the properties of an element into the model. The definitions of the properties and characteristics are done with the help of sections. From the numerous available sections, following types are associated with the current analysis. A section corresponds to a specific material. After identifying section, certain sets of elements are imposed on related section.

1. Beam Section

Beam section is used to define the cross-section for beam elements when numerical integration over the section is required. Girder of the bridge is modeled using I beam section. The integration points for I beam section in stress are shown in figure.

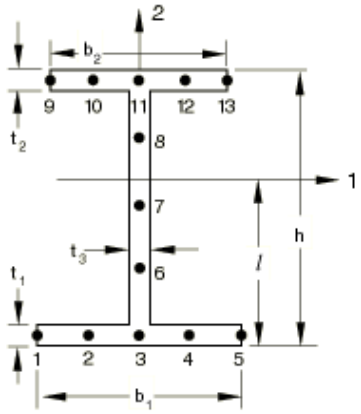

Figure 19: Integration points on I section

2. Shell Section

The use of the shell section is to specify or define a shell cross section in Abaqus input file. The thickness of deck in bridge model is provided using this section.

3. Rebar Layer

For modeling all the steel reinforcement inbuilt rebar element was implemented. In ABAQUS this element is capable of providing embedment within beam or shell elements. Steel Reinforcing rebars are placed in both transverse layer and longitudinal layers within the shell.

4. Rebar

The prestressing rebars in girder are placed using Rebar option.

- **Constraint Elements**

The model built in ABAQUS model is an assembly of individual structural components .Such as beams, shells, studs, etc. Unless these constituent elements are merged to build a bridge, analysis cannot be run. And for joining these elements, constraint elements have to be

employed. The most generally used constraint element used a multipoint Constraint (MPC). A rigid joint simulating a beam is ensured by beam MPC. The simulation is between two nodes. And this simulation is mostly employed for slab and beam elements to generate composite action. The displacement and rotation of one node is directly associated with those of connected node.

3.2.3 Material Properties

Material modeling consists of defining the properties of the different materials used in the structure. Each material definition is actually a combination of various independent characteristics.

- Density
- Elastic Modulus
- Poisson's ratio
- Thermal expansion
- Dependent variables
- User defined field

For accurate results the properties of these materials must be determined and input into the program.

3.2.4 Loading

The research is limited to the effects of dead loads and time-dependent effects.The majority of the loading to be applied in load step are detailed below.

1. Prestress – The prestress is applied as an initial stress to the strand rebars elements.

*INITIAL CONDITIONS, TYPE=STRESS, REBAR

2. Girder Dead Load – A dead load of girder is applied to girder elements.
3. Deck Dead Load – The Deck dead load is applied to the girder elements.

- **Boundary Conditions**

The development of the pinned supports can be done by applying constraint on the x and y planes of the girders cross section.

- **User Subroutines**

As explained in previous chapter user subroutines are used to analyze shrinkage effects in prestressed concrete bridge. They should be included in material property definition of the model. To call UEXPAN user subroutines in input file while analysis is running,

*EXPANSION, USER

is included in material definition.

To call USDFLD user subroutine,

*FIELD, USER

is added at the beginning of each step definition.

3.3 Comparison with Field Data

One of the most important methods to conform the validity of the model used here was to compare it with a reference. The analytical model that was developed here in the project has been validated by the comparison with the data obtained from research titled “Simulation of the Long-Term Behavior of Precast/Prestressed Concrete Bridges – by Eldhose Stephen (2006)”. It is essential to note the details of the bridge that was worked upon for the evaluation in the

aforementioned reference project. The bridge located in New Hampshire, Bristol passing over the Newfound River on the route 104 was taken for the purpose. The geometric and material entities were also defined. The figure below depict the cross sectional segment of the bridge. A precise model was created by extracting required data. Those data which were not available or not clearly stated were presumed to be within the reasonable data to carry the evaluation.

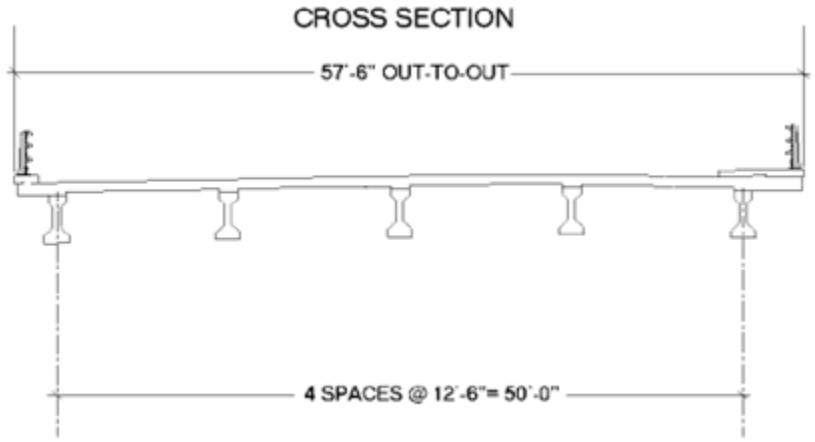

Figure 20: Cross Section of the Bridge (Eldhose Stephen 2006)

Analytical Model

For the simplifying the analysis, a single girder model with a deck was considered. The figure below shows the girder used for modeling which was 150” wide deck with Girder No. 4. The component modeled was 65’ long span of AASHTO type iii girder, its thickness being 9’’ and reinforcement of deck assumed to be 6 #4 bars.

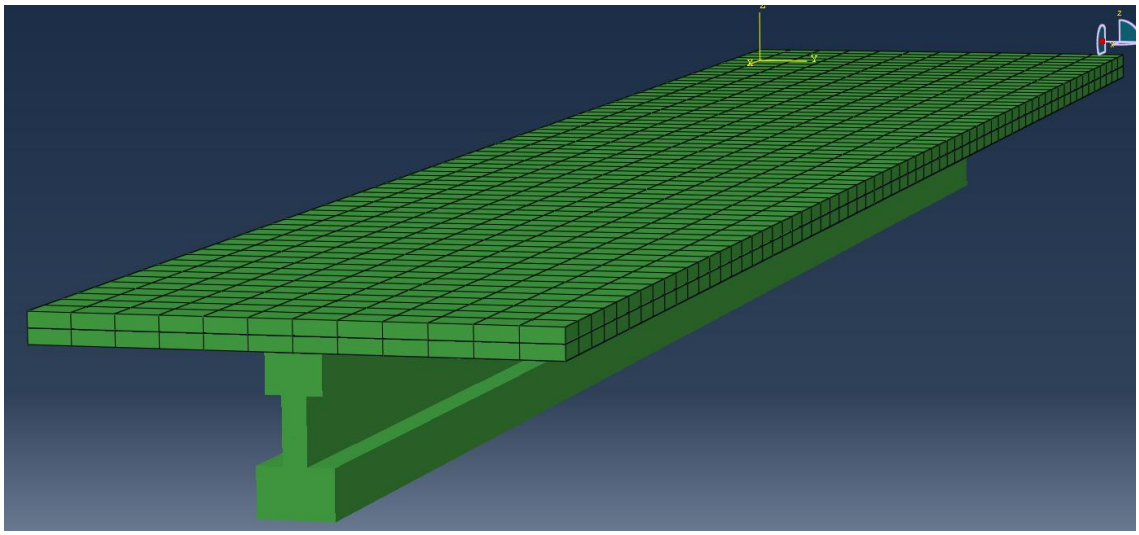

Figure 21: Validation bridge model with single girder

Prestressing strand of grade 270 and diameter 0.5” was identified in girder no 4. In total 40 prestressing strands were placed in 6 layers with 2’’c/c. It is essential to note that the modification in the modeling was done to simplify the analysis. This modified strand pattern has a strand each per layer, and each with greater subsequent cross sectional area. The following table represents the modified strand pattern.

Table 7: Modified Strand Pattern

Layer	Number of Strands	Cross Sectional Area (in^2)	Distance from top of the girder (in)
1	2	0.9815	43
2	2	0.9815	41
3	2	0.5889	39
4	2	0.3926	37
5	2	0.1963	35

The material properties play an important part in behavior and hence also in behavioral analysis. The materials involved in our analysis are Girder concrete, Deck concrete, Rebar steel, and the Prestressing strand steel. The density of girder concrete is 0.148k /ft3. The modulus of elasticity is varying with age as shown in table. Poisson's Ratio has been assumed to be 0.15.

Table 7: Variation of E with respect to Age of Girder

Field Variable = Age (Days)	Modulus of Elasticity (ksi)
1.69	4400
27.8	5050
55.9	5350
365	5850

For deck concrete density is 0.145k/ft3.the elastic modulus as varying with age as shown in table the poisons ratio is assumed 0.15

Table 9: Variation of E with respect to Age (Deck)

Field Variable = Age (Days)	Modulus of Elasticity
7.3	3750
28.1	4250
56.1	4150
122.1	4500

The modulus of elasticity for the steel reinforcement and the rebar can be assumed to be same and it is taken to be 29x106 psi, and Poisson's ratio as 0.25. The tools can be validated using a simply supported structure. The lateral restraints are provided in the deck. An initial stress of 202.5 ksi is applied to the strand elements. A body force of -0.083 lb/in3 applied to the girder elements .A body force of -0.2055 lb/in3 is applied to the girder elements.

Analysis

As discussed in the 2nd chapter of the report, the complete analysis of the above model is done with the help of FORTRAN Subroutines. The behavior of the structure can be examined in detail with the help of Stress and Strain contour plots. Figure below shows contour diagrams of the profile of the girder.

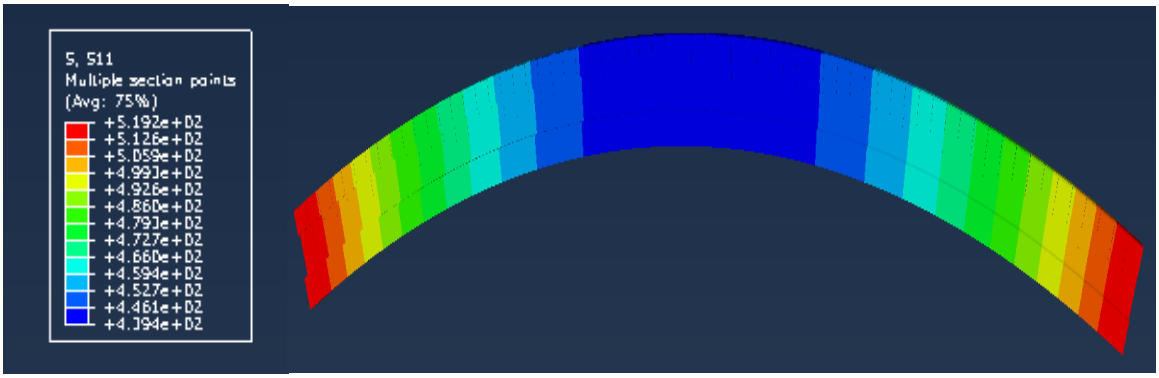

Figure 22: Profile of girder

The stresses in deck is shown figure 22. The development of these stresses can be seen using frames from a Time-History animation of the stress contours. There is a buildup of tensile stress at the center of the deck whereas stress reduction can be seen at the end of the deck.

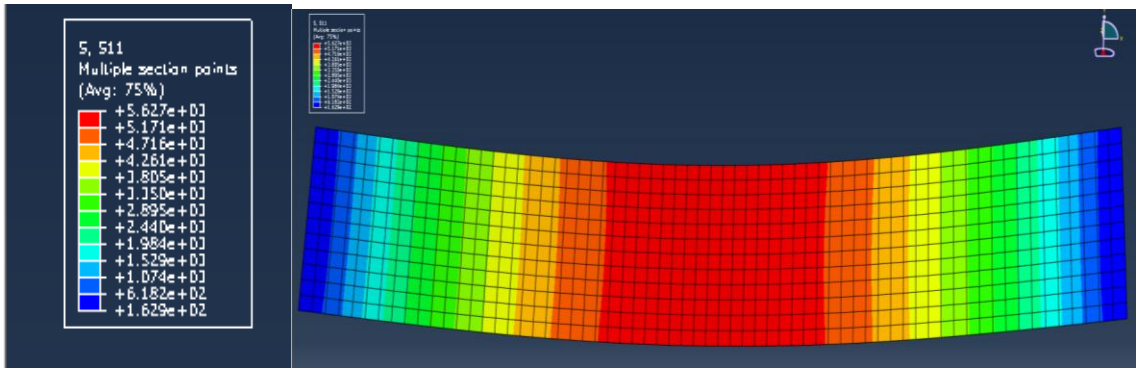

Figure 23: Stress in the Deck

Validation

As mentioned in the beginning of this chapter the validation part is one of the most important parts of this whole research work as it verifies the correctness of the work done. The Abaqus model designed under this research work has been validated by comparing it with the data provided in “Simulation of the Long Term Behavior of Precast/ Prestressed Concrete Bridges” by Eldhose Stephen (2006). One of the most helpful observations of the field results was that of strains. The strains were recorded at three points in the girder on the midspan region. The locations of the points are 41”, 37”, and 33.2” below the top of the girder. The strain patterns at all these locations are depicted in the figure below. The total strain patterns are plotted using XY data tool for a node at midspan. A general pattern of the curve has been identified with some common features among them. These common things are

1. Increase in strain due to the release of prestress combined with Girder Dead Load.
2. Creep induced progressive increase in strain
3. Spontaneous fall in strain because of deck dead load
4. Steady increase in strain because of a joint effect of creep & differential shrinkage

A spontaneous upward camber is generated because of prestress release which is backed by a progressive enhancement because of action of creep. It is to be noted here that after pouring of deck, the effect of passive loading decreases the camber. After this reduction hardly any changes are observed.

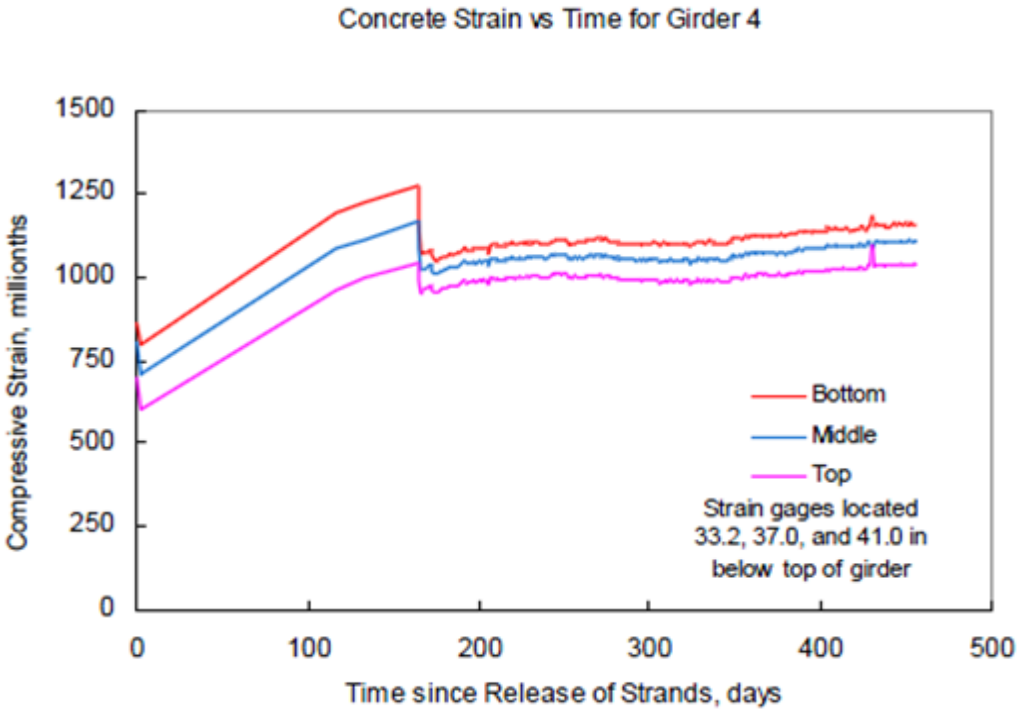

Figure 24: Strain Data from FHWA observations (FHWA 2001)

The graph is plotted for middle strain gage. Using OBD output XY data is plotted for a node in girder section. The comparison graph is plotted below. The graph shows result obtained from FEM and strain data from field.

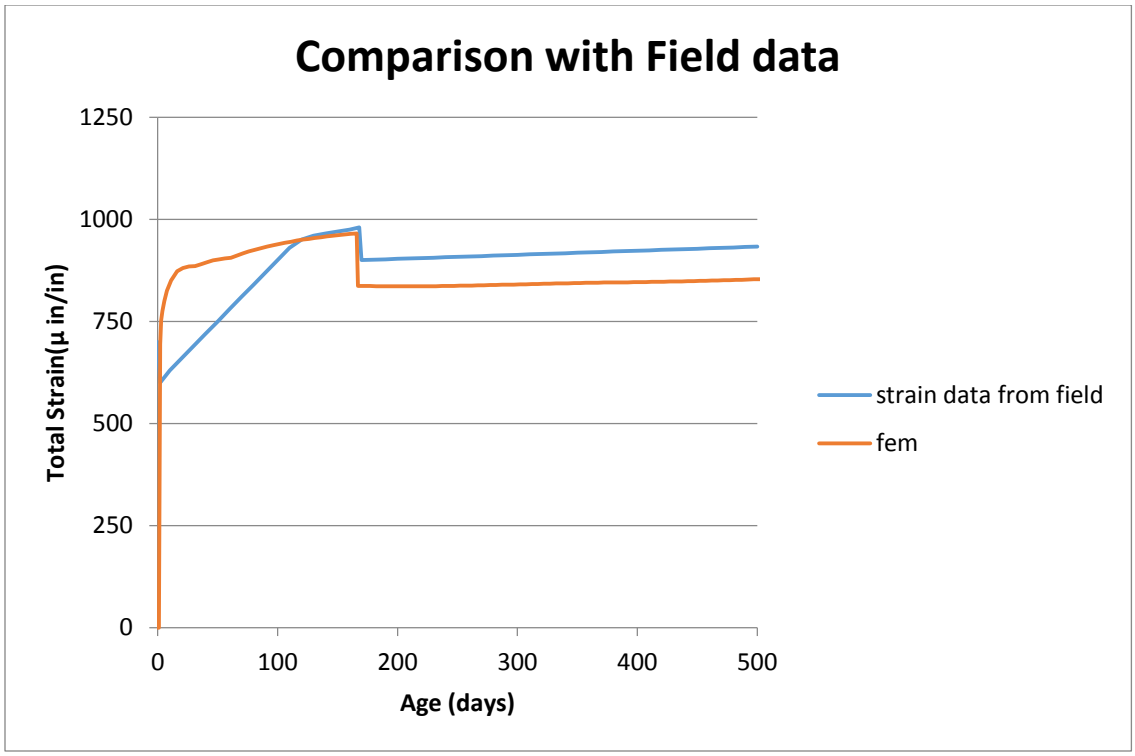

Figure 25: Comparison graph with field data

The outcomes of the analysis are found to be matching with the observations documented in the FHWA report. This analogy is significant enough to ensure the capability of Abaqus model to accurately simulate the behavior of prestressed concrete bridges.

CHAPTER 4

Results

This chapter comprises of the results obtained from the analysis with the help of Abaqus software. The section specifically addresses the results of the parametric study that was carried out as explained in the previous section. This section is discussed with the help of the figures of modeled bridges in Abaqus. As mentioned earlier group of bridges were selected and put under the analysis to identify the exact effects of a particular parameter.

4.1 Results of bridge 1

Bridges are modeled in Abaqus as explained in previous chapter. After modeling the bridge analysis is carried out in visualization module in Abaqus. Using ODB field output XY data plot can be carried out. The stress and strain contours are plotted. To find out stress or strain at particular point, section point option is used.

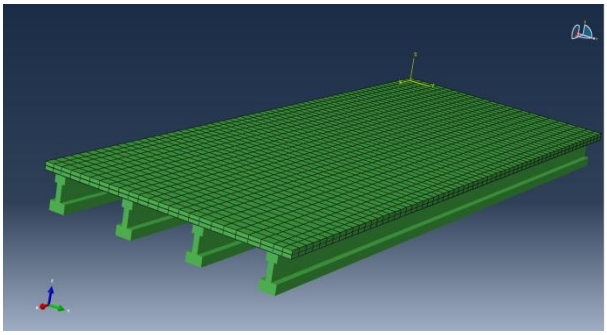

Figure 26: Abaqus model of Bridge 1

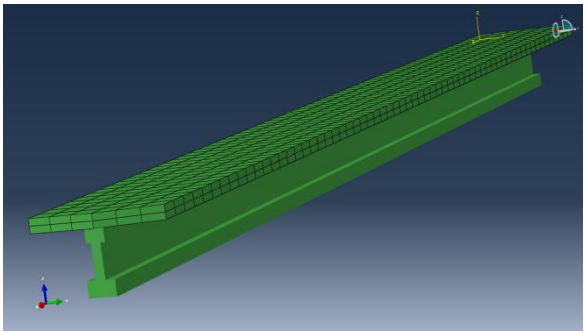

Figure 27: Abaqus Model of Bridge 1 with single girder

Figure 26 and figure 27 represent the bridges model on single girder that were done in Abaqus. Bridge 1 is modeled with single girder as shown in figure 27 and analysis is carried out in visualization module. The stress contours are plotted in top and bottom of the deck as shown in figure 28 and figure 29.

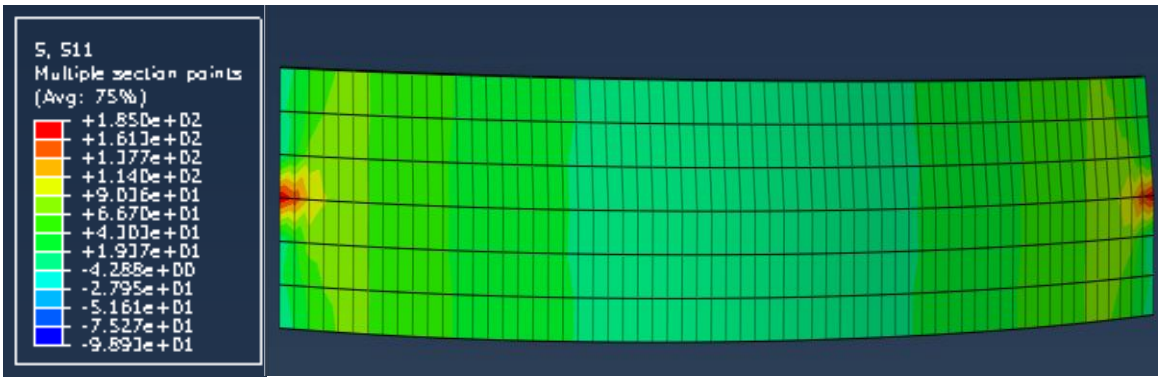

Figure 28: Stress in top of the deck

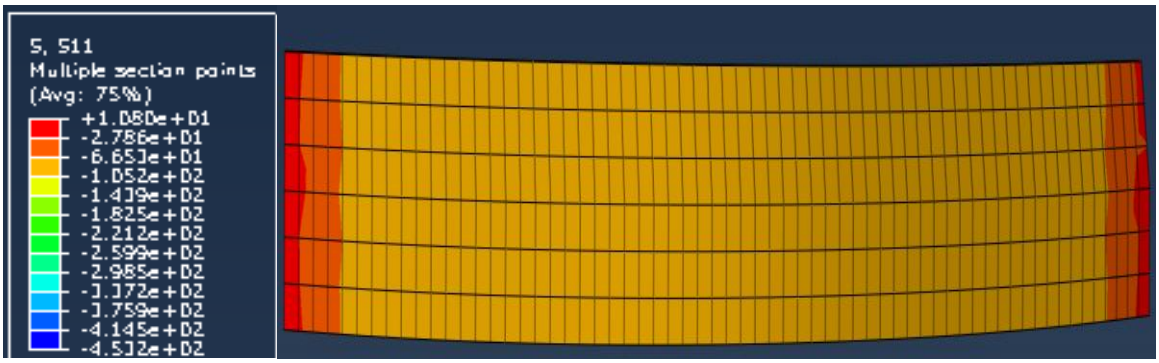

Figure 29: Stress in bottom of the deck

Stress in top of the deck is greater than the stress in bottom of the deck. The strain contours in girder is also plotted. Figure 30 shows the shrinkage strain contours in girder.

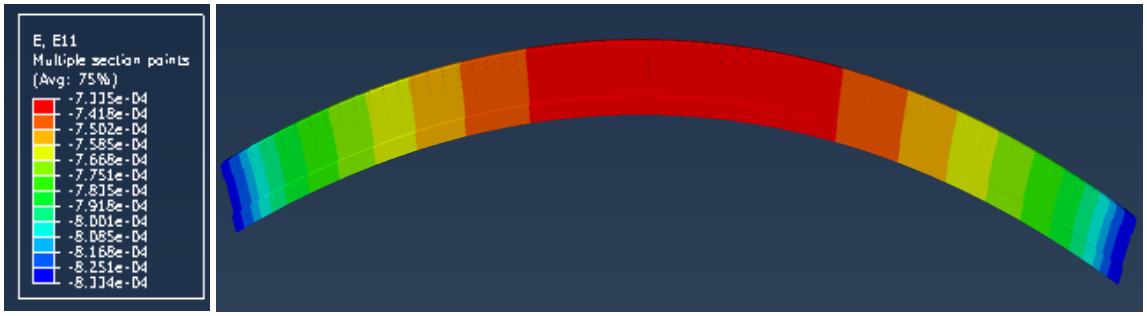

Figure 30: Shrinkage in girder

Here, analysis is done using single girder instead of whole bridge. The effect of whole bride can be seen by giving lateral restraint to the single girder bridge. The lateral restrained are provide to Bridge 1. Stress contours are plotted to see the stress results on the bridge deck. The stress in top and bottom of the deck can be seen in Figure 31 and figure 32.

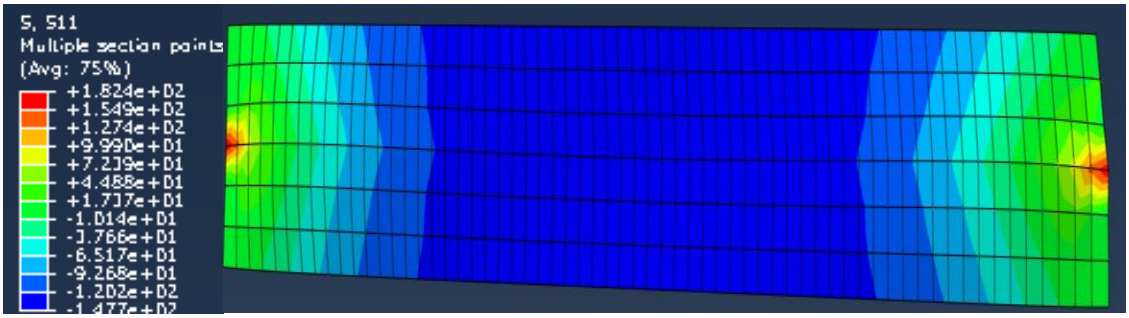

Figure 31: Stress in top of the deck

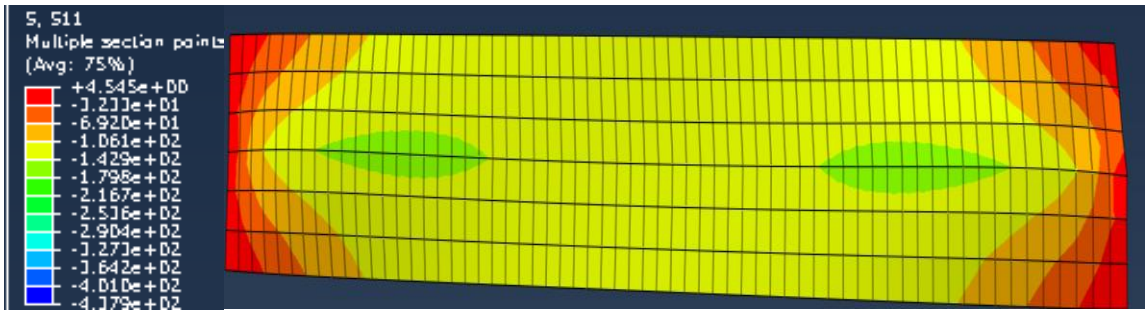

Figure 32: Stress in bottom of the deck

4.2 Parametric Study Results

It was explained in the previous chapter how the selection of variables and the procedure for the selection of bridges. The parametric study with respect to selected four variables was carried with a view to reaching a specific conclusion in terms of dependability of shrinkage with respect to that particular parameter. The analysis was carried out using Abaqus and the results were thoroughly evaluated. In this segment results are depicted with the help of graphs of Strain with respect to Time (Days). The results are documented in a similar manner to that of explanation for details of the parametric data base. In the following section, the obtained graphs are represented with respect to the factor of parametric study.

1. Results for parametric study with respect to Length

Four bridges were modeled to see the effect of length of the span on shrinkage pattern. The study of these graphs represents the nature of the changes that occurs in the structure with changing length. 80ft and 100 ft long span bridge with girder spacing of 6 ft are modeled .The stress contour in 80 ft long span and 100 ft long span are shown in figure 33 and figure 35. The strain contours are also plotted in top of the deck in 80 ft and 100 ft long span bridge as shown in figure 34 and figure 36.

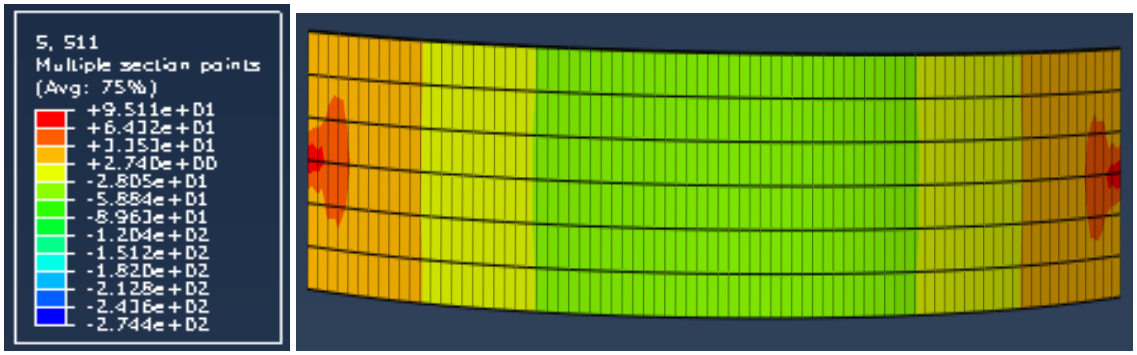

Figure 33: Stress at top of the Deck for 80 ft span

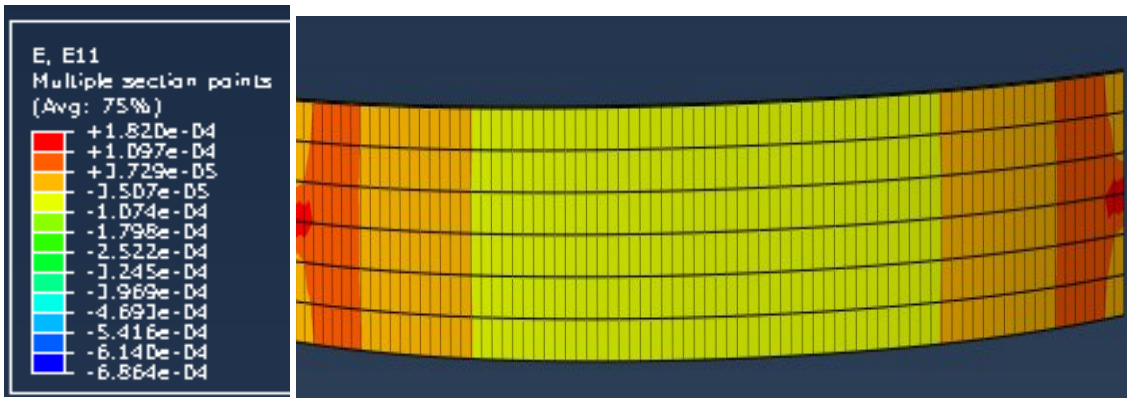

Figure 34: Shrinkage in top of the Deck for 80 ft span

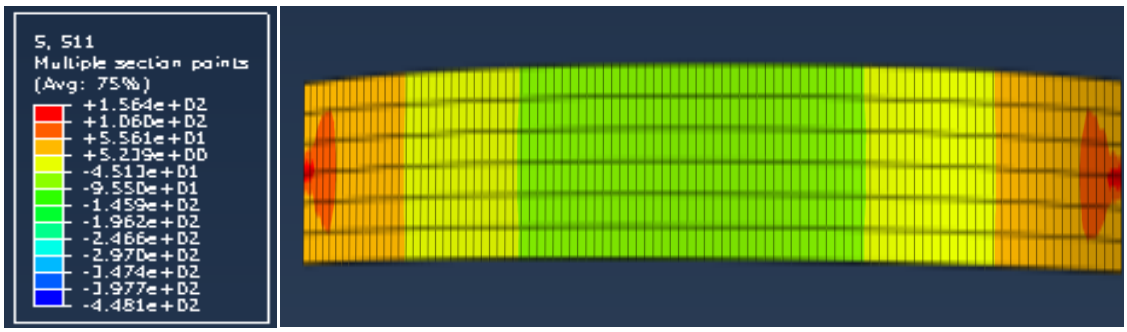

Figure 35: Stress in top of the Deck for 100 ft span

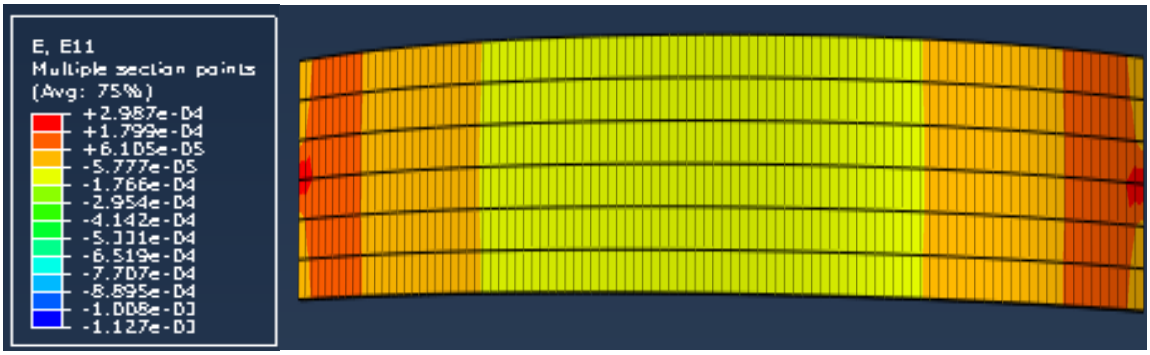

Figure 36: Shrinkage in top of the Deck for 100 ft span

It can be inferred that the stress and strain in the deck increases with the length of the span. The stress in bridge withspan length 80 ft has lower stress then the stress in bridge with 100ft span. There is also observed a change in shrinkage strain in deck with change in span length. The following graph refers to the first group of the bridges detailed in the previous chapter. The strain versus time graph is plotted using OBD field output. The XY graph is plotted at integration point 1 in both the bridge in the middle of the girder. The strain in bridge with 100 ft span length has been found to be greater over time period according to figure 37. That follows that the shrinkage in 100ft span bridge is greater than 80 ft span bridge.

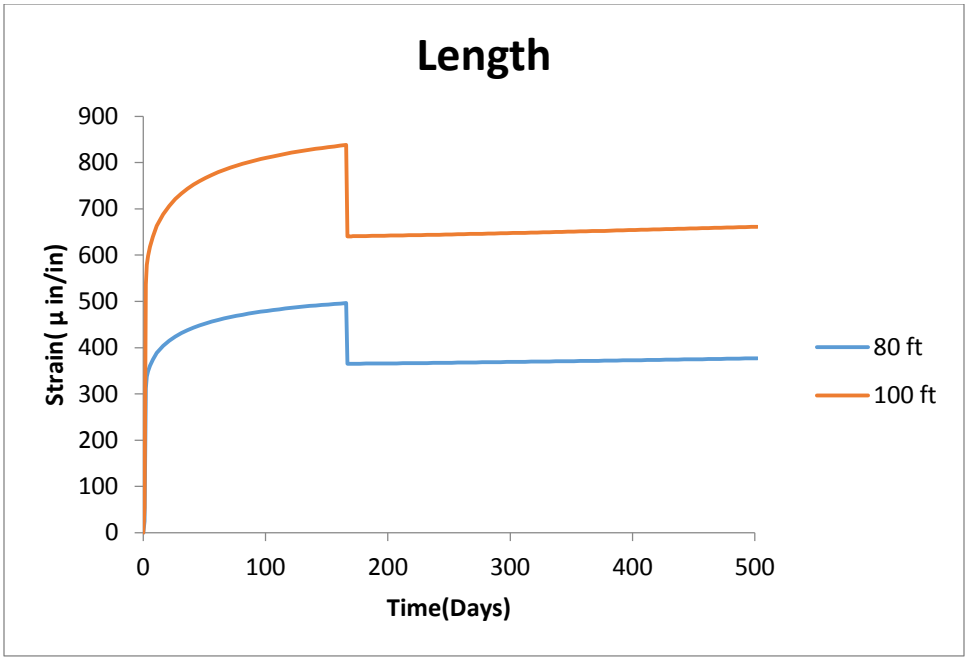

Figure 37: Comparison of Strain in girders for span length 80 ft and 100 ft

For the other two bridges of the group, 60ft and 80 ft long span bridge with girder spacing of 10 ft are modeled. The stress contour in 60 ft long span and 80 ft long span are shown in figure 38 and figure 40. The strain contours are also plotted in top of the deck in 60 ft and 80 ft long span bridge as shown in figure 39 and figure 41.

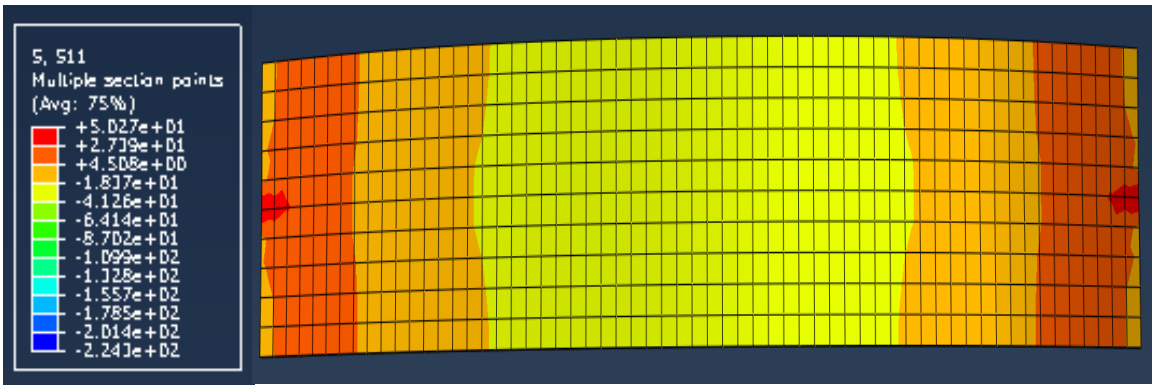

Figure 38: Stress in top of the deck for 60 ft span

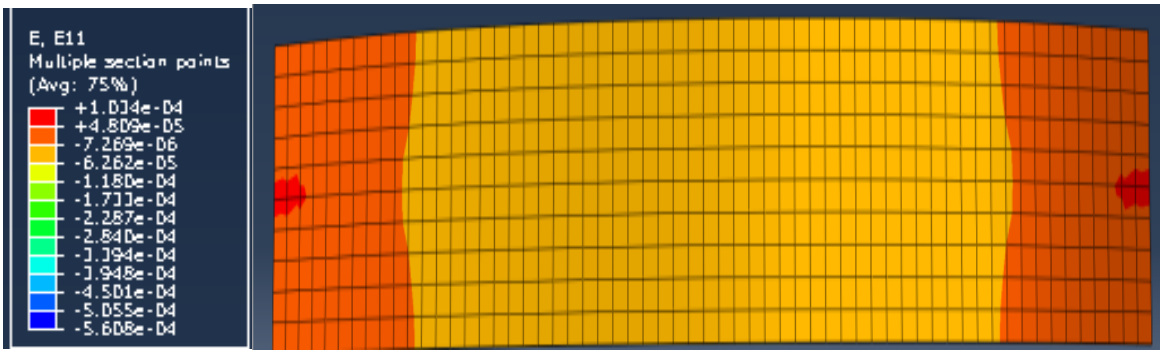

Figure 39: Shrinkage strain in top of the deck for 60 ft span

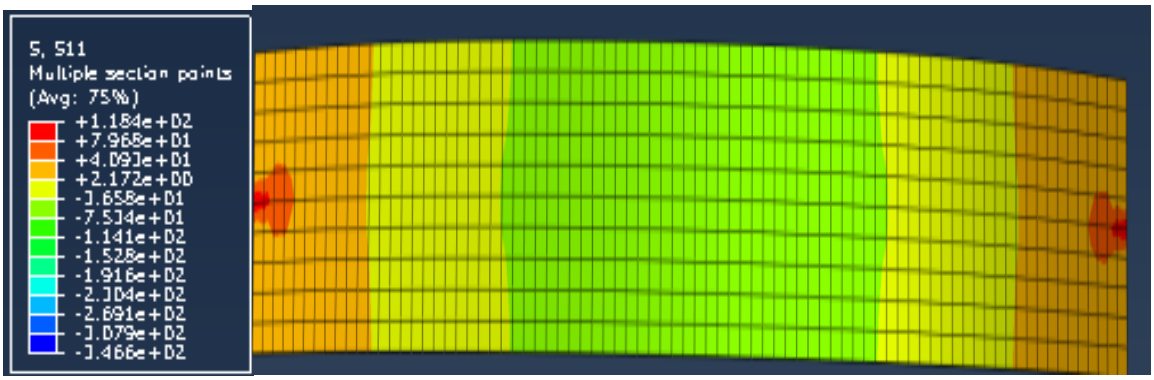

Figure 40: Stress in top of the deck for 80 ft span

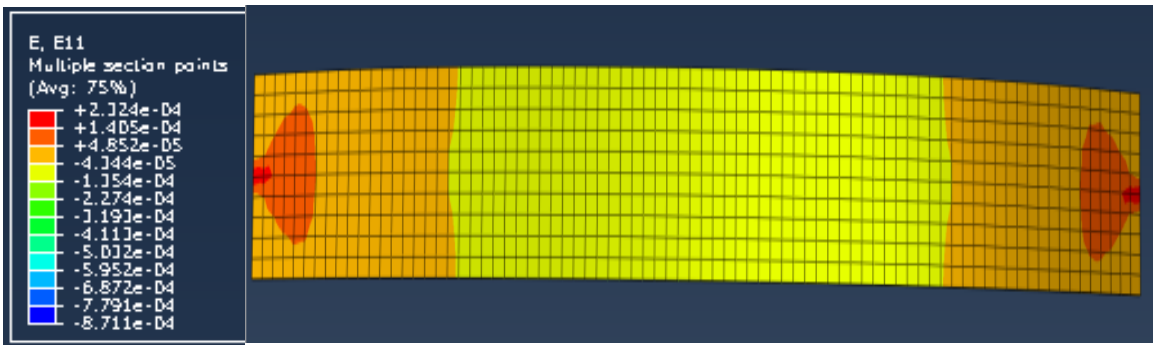

Figure 41: Shrinkage in top of the deck for 80 ft span

For these two bridges as well the previous observation holds true. The stress and strain in the deck increases with the length of the span. Moreover similar to the earlier remark the stress in bridge withspan length 60 ft has lower stress than the stress in bridge with 80ft span. The shrinkage strain in deck is also changing with span length. The XY graph is plotted at integration point 1 in both the bridge in the middle of the girder. The strain in bridge with 80 ft span length is greater over time period according to figure 42. Thus shrinkage in 80 ft span bridge is greater than 60 ft span bridge.

It can be inferred from the above two observations that an increase in a bridge length also increases shrinkage in the bridge structure.

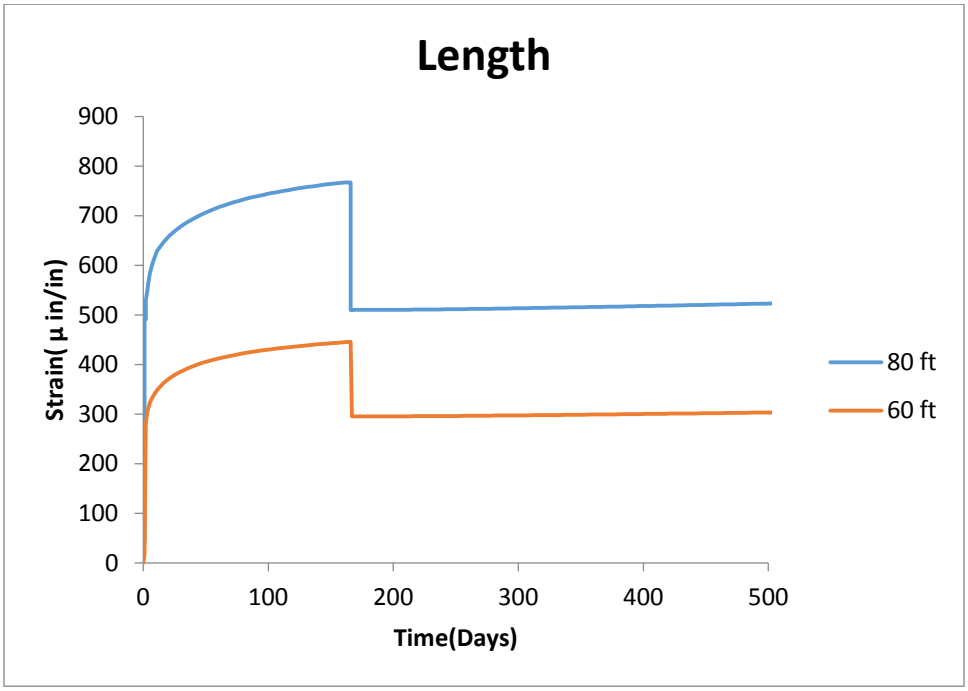

Figure 42: Comparison of Strain in girders for span length 60 ft and 80 ft

2. Results of parametric study with respect to Girder Spacing

One of the major factors that affect the nature of shrinkage relatively is girder spacing. The results represented here in this section explain the behavior of shrinkage patterns relative to girder spacing. Three bridges were model to see the effect of girder spacing. Three bridges with constant span length (80 ft) were modeled for girder spacing of 6 ft, 8 ft and 10 ft. The stress contour for 6ft, 8 ft and 10 ft girder spacing are shown in figure 43, figure 45 and figure 47 respectively. The strain contours are also plotted in top of the deck of bridge for all three bridges and are depicted in the figure 44, figure 46 and figure 48.

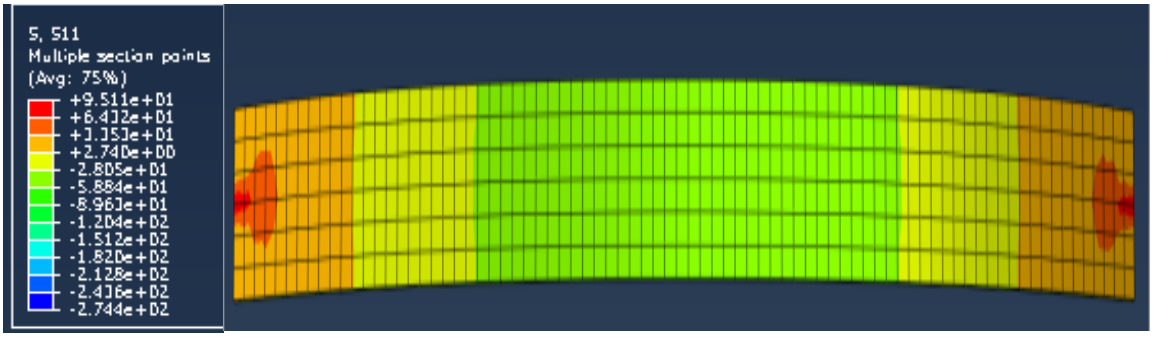

Figure 43: Stress in top of the deck for 6 ft spacing of girder

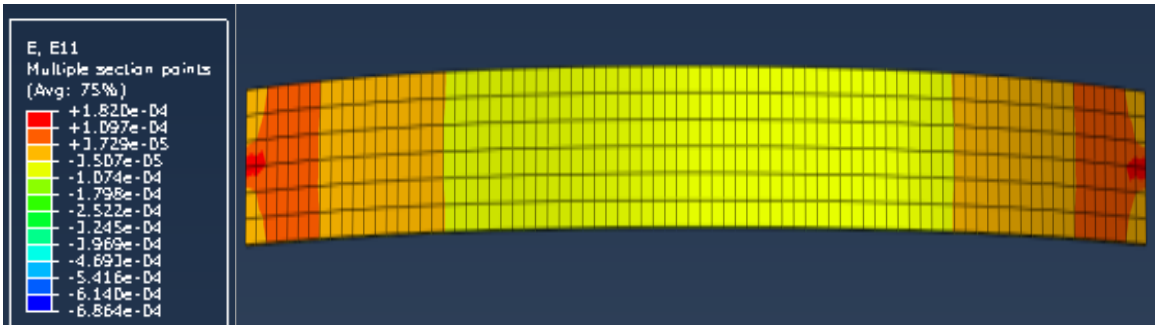

Figure 44: Shrinkage in top of the deck for 6 ft spacing of girder

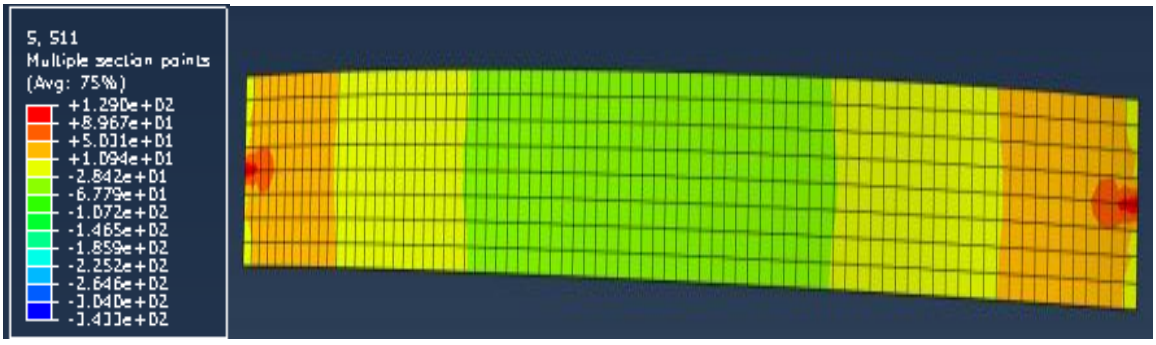

Figure 45: Stress in top of the deck for 8 ft spacing of girder

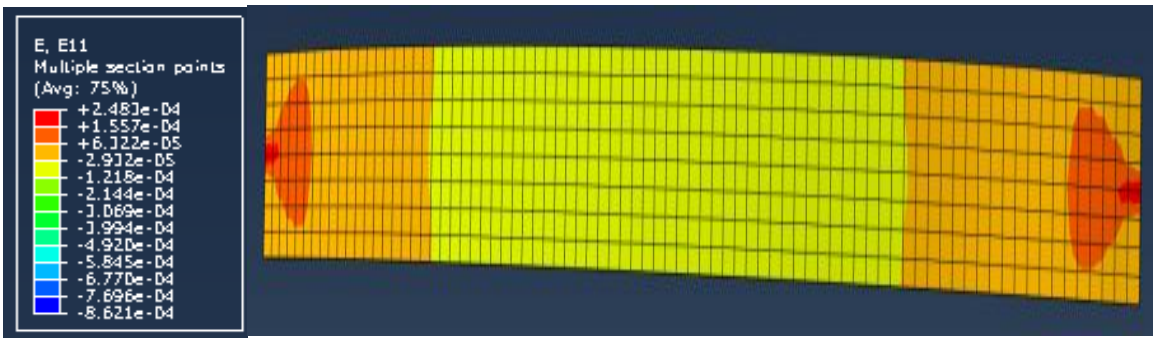

Figure 46: Shrinkage in top of the deck for 8 ft spacing of girder

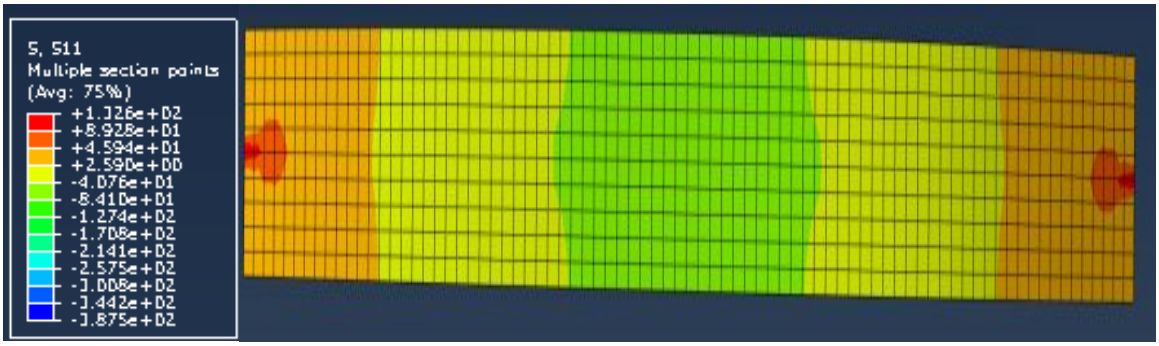

Figure 47: Stress in top of the deck for 10 ft spacing of girder

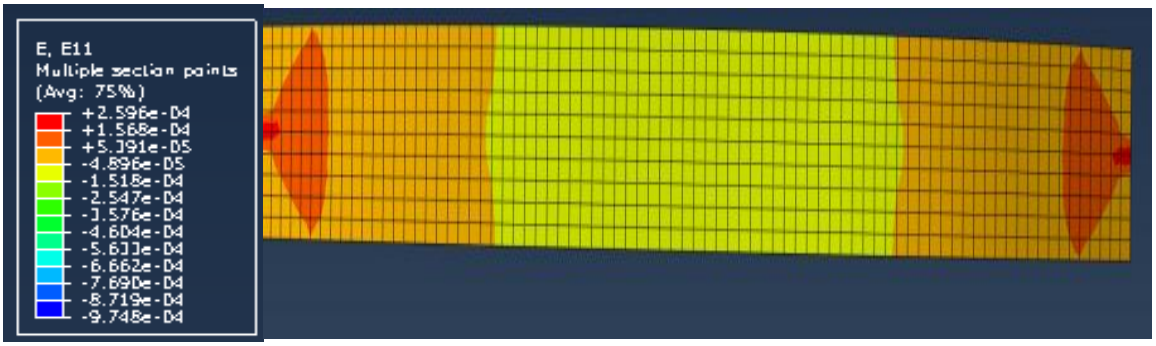

Figure 48: Shrinkage in top of the deck for 10 ft spacing of girder

It can be noticed that the stress and strain follows the change in girder spacing. And this change is in direct proportion, meaning an increase in girder spacing also results in increase in the stress and strain in the deck. The stress in bridge with girder spacing of 6 ft has lower stress than the girder spacing of 8ft. And that for bridge with 8 ft girder spacing is less than that for bridge with 10 ft girder spacing. The shrinkage strain in deck is also changing with girder spacing. The XY graph is plotted at integration point 1 in both the bridge in the middle of the girder. The strain in bridge with 10 ft girder spacing has greater over time period as can be seen in figure 49. The shrinkage in bridge with girder spacing of 8 ft is greater than that in bridge with 6 ft girder spacing.

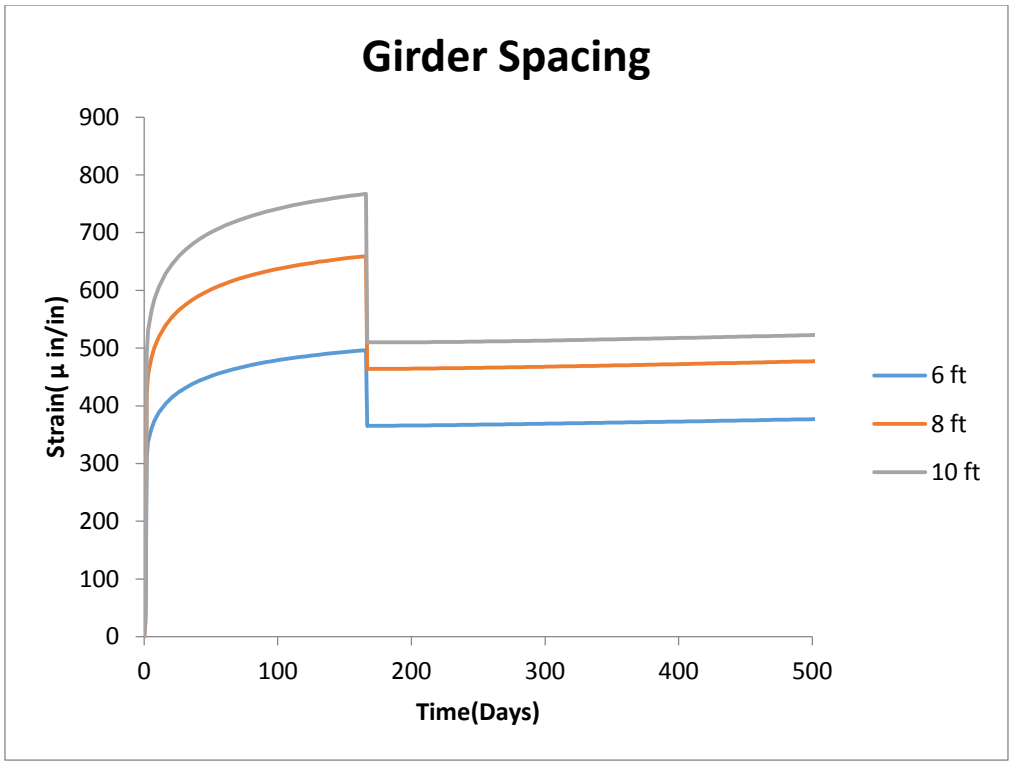

Figure 49: Comparison of Strain in girders for girder spacing of 6 ft, 8 ft and 10 ft

Thus it can be inferred that the shrinkage in the bridge structure increases with the increase in the girder spacing of the bridge.

3. Results of the parametric study with respect to Deck Thickness

It was desirable to find out the effects of change on deck thickness on shrinkage and related properties. The results obtained are recorded below. Three bridges were model to see the effect of deck thickness on shrinkage behavior of the bridge. Three bridges with a constant span length of 100 ft were modeled for various deck thickness valued 6in, 8 in and 10 in. The stress contour for bridges with deck thickness of 6in, 8 in and 10 in are shown in figure 50, figure 52 and figure 54. The strain contours are also plotted in top of the deck of bridge for all three bridges and are shown in figure 51, figure 53 and figure 55.

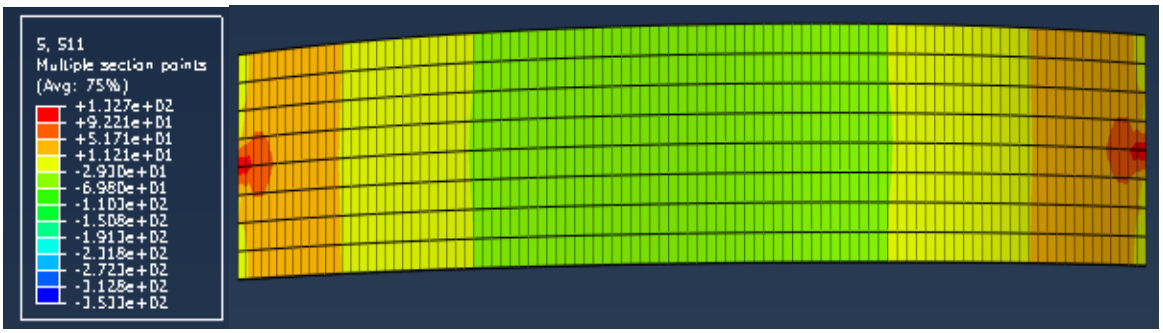

Figure 50: Stress in top of the deck for 6 in thickness of deck

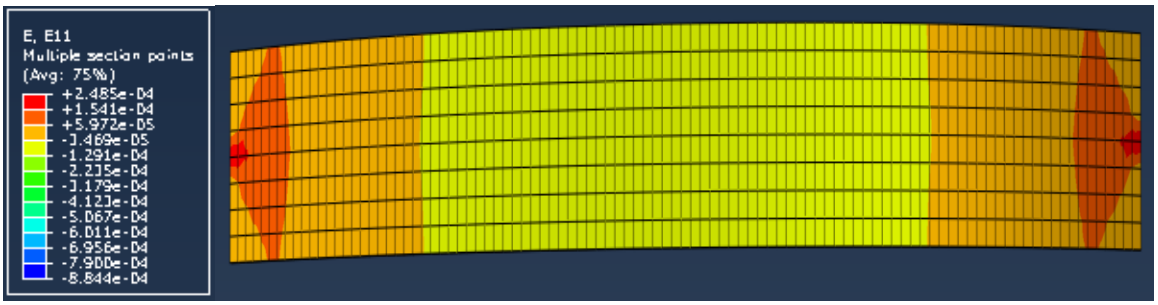

Figure 51: Shrinkage in top of the deck for 6 in thickness of deck

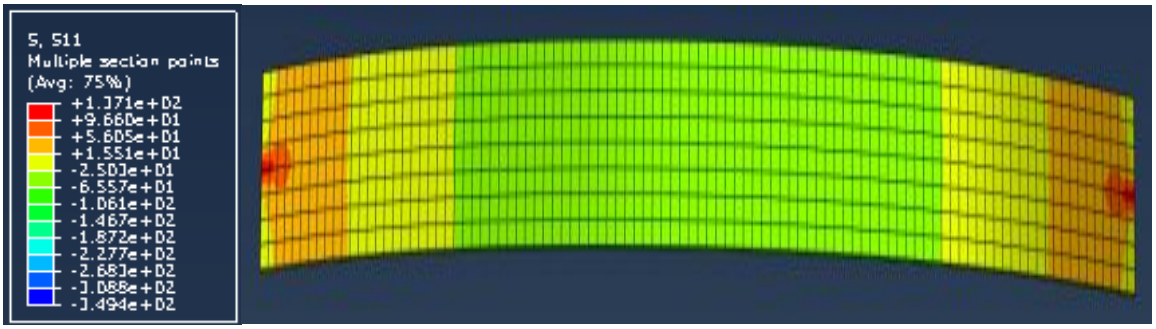

Figure 52: Stress in top of the deck for 8 in thickness of deck

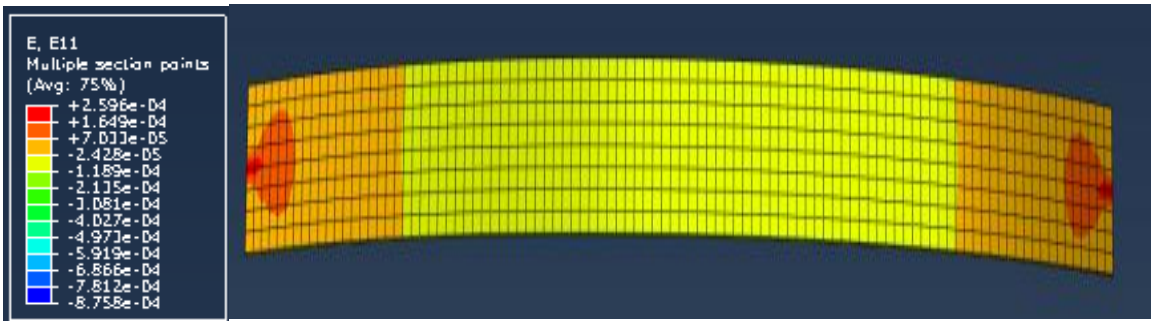

Figure 53: Shrinkage in top of the deck for 8 in thickness of deck

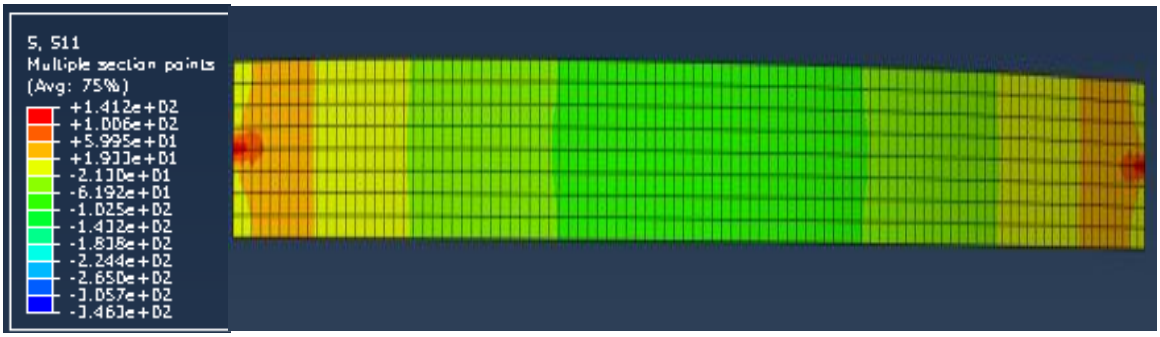

Figure 54: Stress in top of the deck for 10 in thickness of deck

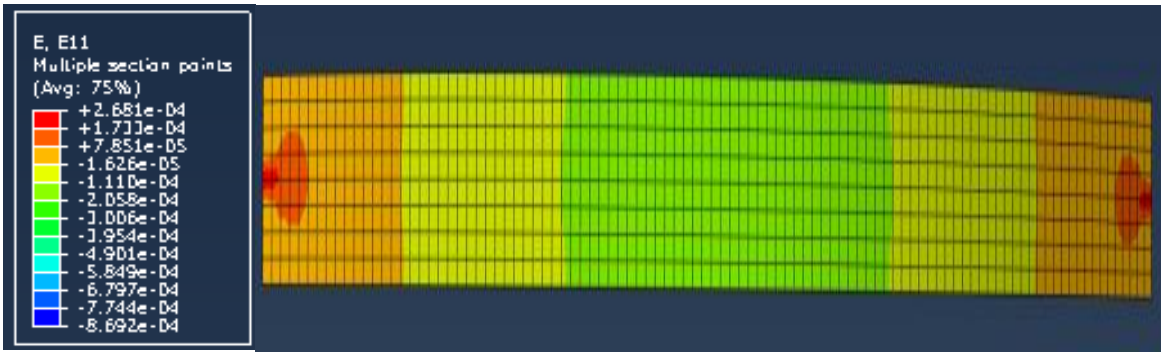

Figure 55: Shrinkage in top of the deck for 10 in thickness of deck

The stress and strain in the deck were found to be decreasing with increase in thickness of deck. The stress in bridge with thickness of 8 in has higher stress then the bridge with 10 in deck thickness. Reportedly the stresses in bridge with 10 ft deck thickness is lower than in the bridge with 8 in and 6 in deck thickness. The shrinkage strain in deck is also changing with slab thickness. The XY graph is plotted at integration point 1 in both the bridge in the middle of the girder. The strain in bridge with 6 in deck thickness is found to be more over time period according to figure 56. The shrinkage in bridge with 8 in deck thickness is greater than that with 10 in. This suggests an inverse relation between deck thickness of the bridge and shrinkage.

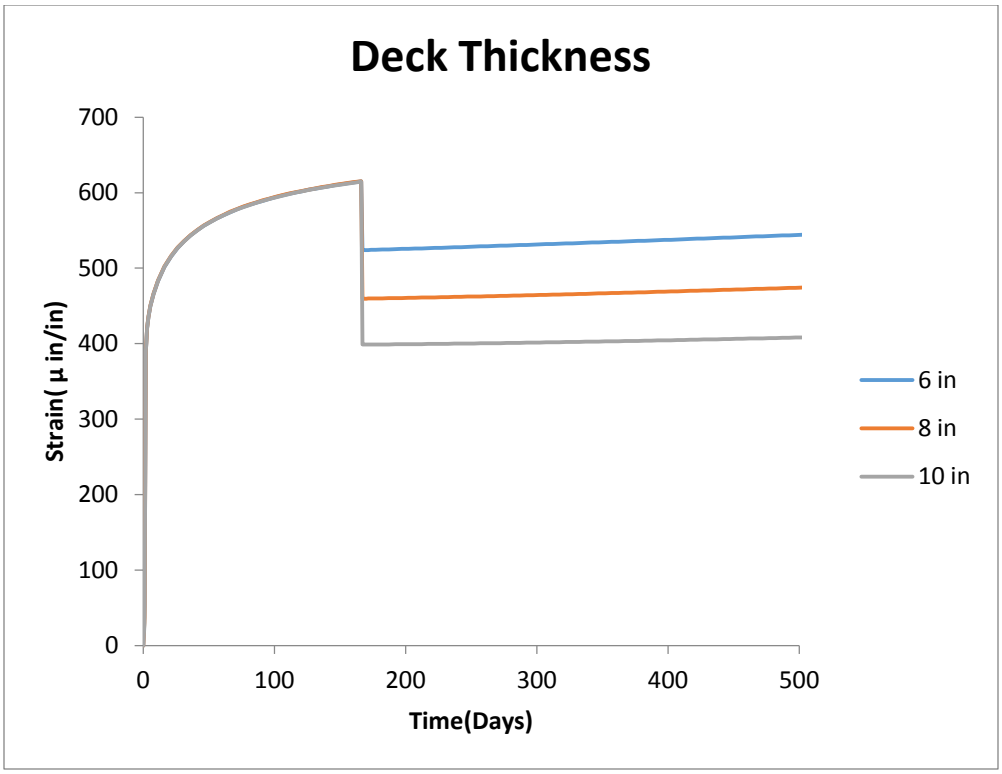

Figure 56: Comparison of Strain in girders with deck thickness of 6in, 8 in and 10 in

It is thus obvious that the larger the deck thickness the lesser is the shrinkage. Thus in other words shrinkage decreases with increase in the deck thickness.

4. Results of parametric study with respect to Compressive Strength of Girder

Apart from the geometric properties listed and their effects discussed above, compressive strength of the girder was found to be significantly powerful entity to affect the shrinkage pattern. The analysis in this respect provides a window for selection to engineers. Three bridges were model to see the effect of compressive strength of girder. Three bridges with span length of 60 ft were modeled for compressive strength of 6 ksi, 8 ksi and 10 ksi. The stress contour for 6 ksi, 8 ksi and 10 ksi compressive strength are shown in figure 57, figure 59 and figure 61. The strain contours are also plotted in top of the deck of bridge with 6ksi, 8 ksi and 10 ksi compressive strength of girder as shown in figure 58, figure 60 and figure 62.

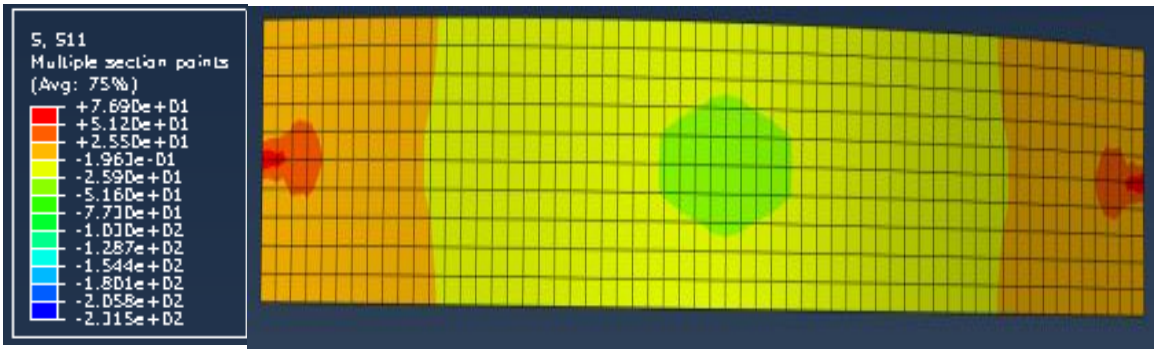

Figure 57: Stress in top of the deck for 6 ksi compressive strength

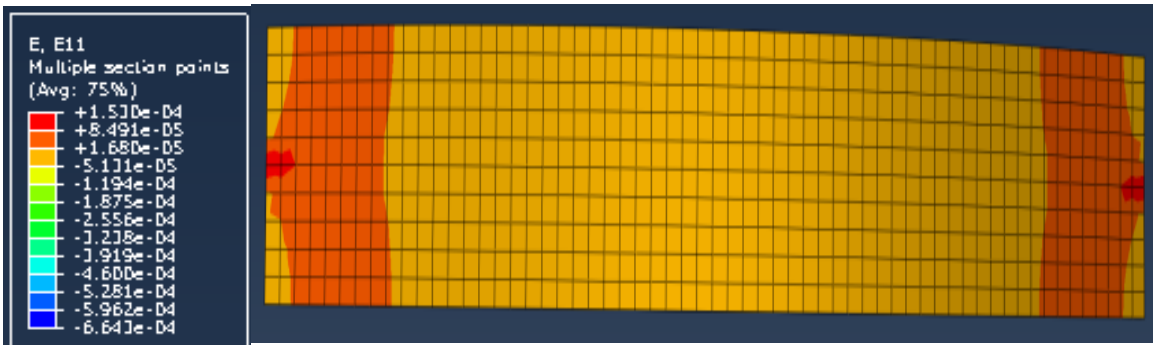

Figure 58: Shrinkage in top of the deck for 6 ksi compressive strength

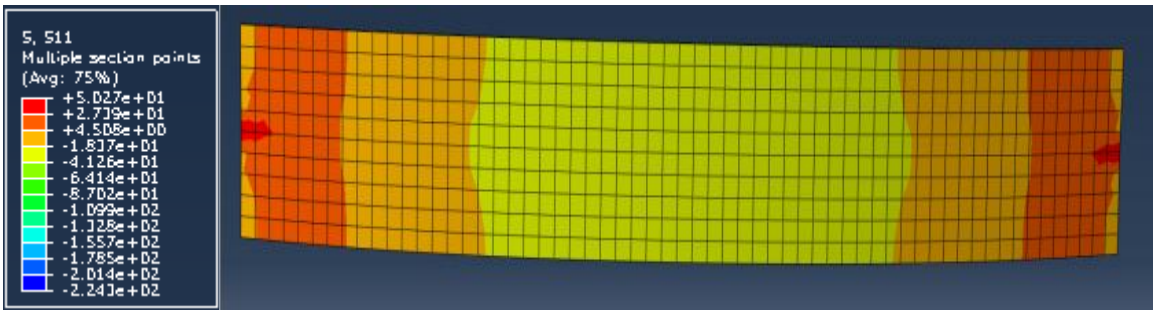

Figure 59: Stress in top of the deck for 8 ksi compressive strength

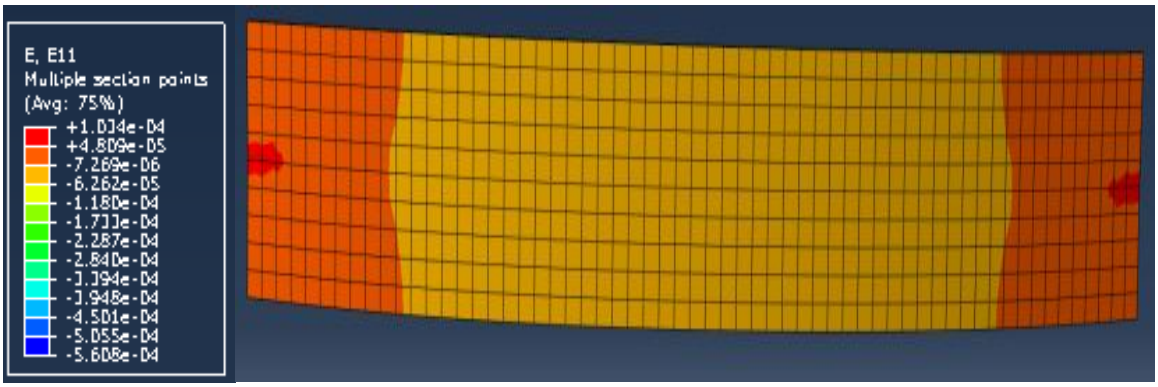

Figure 60: Shrinkage in top of the deck for 8 ksi compressive strength

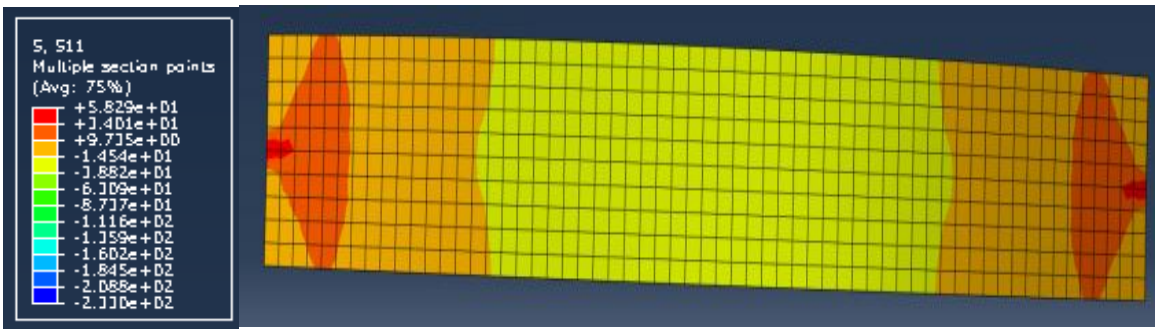

Figure 61: Stress in top of the deck for 10 ksi compressive strength

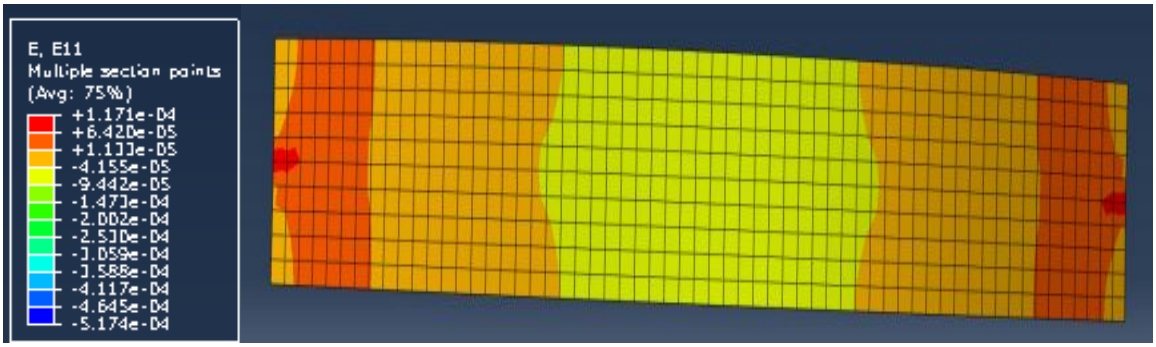

Figure 62: Shrinkage in top of the deck for 10 ksi compressive strength

The stress and strain in the deck were found to be decreasing with increase in compressive strength of girder concrete. The stress in bridge with compressive strength of 8 ksi has higher stress then that with 10 ksi compressive strength of girder. The stress in bridge with 10 ksi compressive strength is lower than 8 ksi and 6 ksi compressive strength of girder. The shrinkage strain in deck also found varying with compressive strength of girder. The XY graph is plotted at integration point 1 in both the bridge in the middle of the girder. The strain in bridge with 6 ksi compressive strength is greater over time period as can be seen in figure 63. The shrinkage in 8 ksi compressive strength is greater than 10 ksi compressive strength. Hence, higher compressive strength of girder will decrease shrinkage strain.

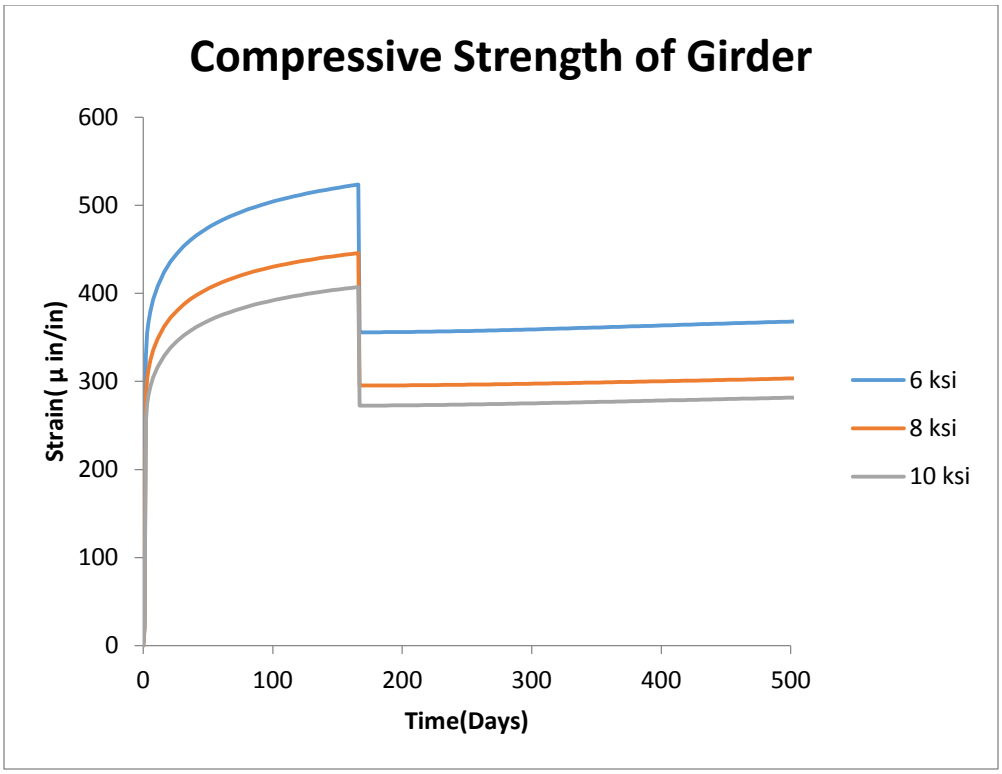

Figure 63: Comparison of Strain in girders for compressive strength of 6 ksi, 8 ksi and 10 ksi

5. Results of the parametric study with respect to Restrained Condition

It was desirable to find out the effects of change on restrained conditions on shrinkage in deck. The results obtained are recorded below. Three bridges were model to see the effect of restrained condition on shrinkage behavior of the bridge. Three bridges with a constant span length of 80 ft were modeled for various boundary conditions as pinned-roller, pinned –pinned and fixe-fixed. The strain contours are plotted in top of the deck of bridge for all three bridges and are shown in figure 64, figure 65 and figure 66.

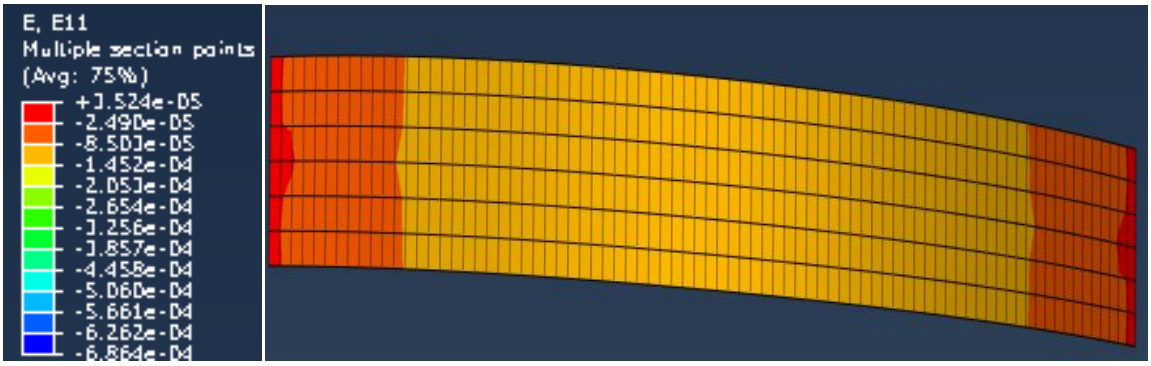

Figure 64: Shrinkage strain in top of the deck with pinned –roller boundary condition

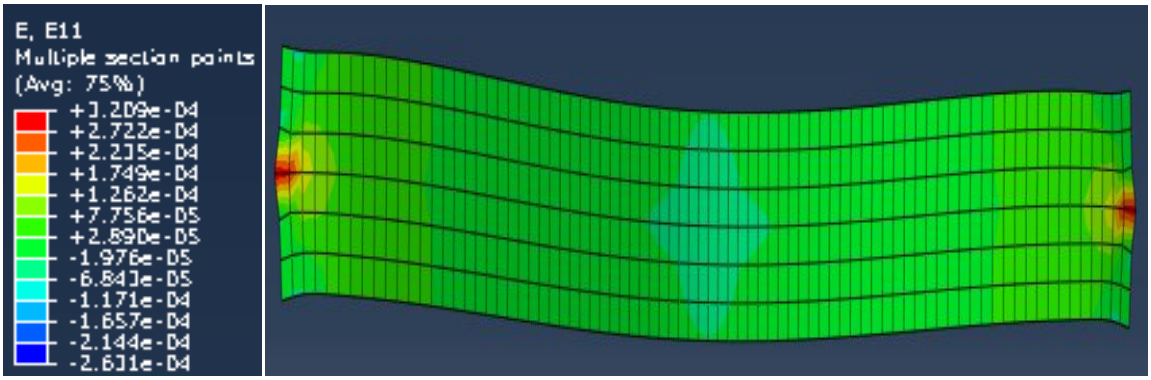

Figure 65: Shrinkage strain in top of the deck with pinned –pinned boundary condition

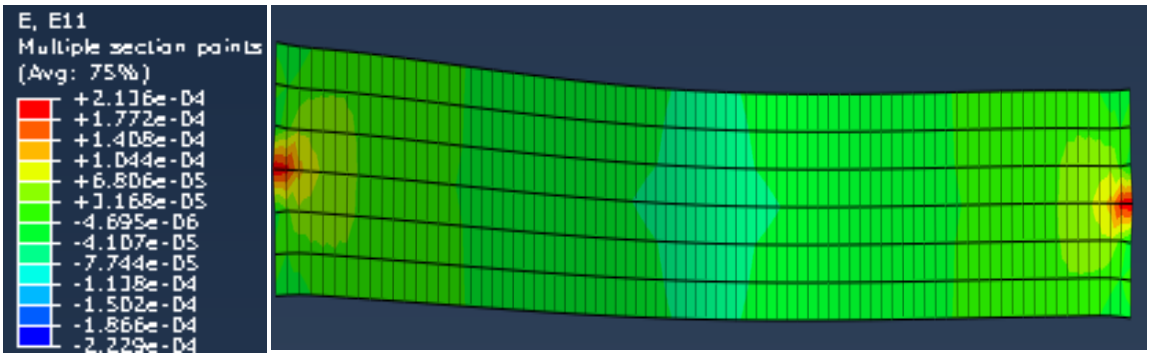

Figure 66: Shrinkage strain in top of the deck with fixed –fixed boundary condition

The strain in the deck were found to be increasing when the deck is more restrained. The shrinkage strain in deck also found varying with compressive strength of girder. The shrinkage strain contour lines are showed in fig. The strain in bridge with fixed boundary condition at both ends is greater as can be seen in figure 66. The shrinkage in bridge with pined boundary conditions at both ends is greater than bridge with pinned –roller boundary conditions. Hence, shrinkage will increase with increased restrained of girder.

CHAPTER 5

Conclusions

5.1 Conclusions

The overall research has been carried for the purpose of incorporating the time dependent Shrinkage Effects into FEM using ABAQUS software. The research has successfully carried its purpose. The ability of ABAQUS to proficiently evaluate the behavior of the prestressed concrete with respect to time dependency is thoroughly justified. The results discussed in the previous chapter corroborate the approach of using Finite Element Method for precise evaluation of the behavior of the prestressed concrete bridge. The major objective of the research to carry a parametric study of the factors that affect the shrinkage effects has been successfully achieved. The results described in the previous chapter present an analytic view of the parametric study. The following synopsis can be documented at the end of this research work in the context of the objectives and the analysis of prestressed concrete bridge and FEM analysis.

This segment of the conclusion chapter has been categorized into two segments. One representing conclusive observations for concerning software and the other concerning parametric study of prestressed concrete bridges.

- Software Conclusions

Creep and shrinkage effects are very important in the analysis of the concrete structure. In Abaqus material modules do not directly provide the provisions for incorporating shrinkage in

concrete. But the provision of the user defined features provides a way to include time dependent effects into the software and run analysis. This research does serve as the demonstration of how successfully Abaqus can incorporate time dependent events and or factors with the help of “user defined” provision of the software. It hence have been justified that the user friendly Abaqus can and should be used for accurately predicting shrinkage behavior in prestressed concrete bridges relative to various factors.

- Parametric Study of Prestressed Concrete Bridge Conclusions

The conclusions based on the results obtained in the research and discussed in the previous chapter can be summarized as mentioned below.

1. Length – The longer the span the greater the Shrinkage
2. Girder Spacing – The Shrinkage strain depends directly on girder spacing.
3. Deck Thickness – The deck thickness inversely governs the shrinkage in the deck.
4. Compressive Strength of girder – The greater the compressive strength of girder the lesser the shrinkage in the bridge.
5. Restrained- Shrinkage strain is increasing with restrained girder.

Above conclusions are drawn directly from the results obtained in the parametric studies of shrinkage with respect to five chosen parameters.

5.2 Future Investigation

This research has only taken into considerations the basic requirements of a model for a bridge and therefore, further investigation is required to explore the full potential of Abaqus and also the complete detailed analysis of various factors affecting shrinkage in prestressed concrete bridges. The concept can also be extended to the other structures built on similar technology and analysis can be done for these structures as well. Below are some suggestions of possible improvements to the model.

1. Daily temperature variations can be applied by temperature gradients. And hence creep and shrinkage would have to be applied as part of the temperature field or as a function of temperature field.
2. The various factors affecting creep coefficient and ultimate shrinkage, as per ACI Committee 209 can be included in the user subroutine.
3. Live loads may be applied to the structure and their intensity can be varied using the amplitude facility.

REFERENCES

1. PCI Design Handbook, Edition 6th, Precast and Prestressed Concrete, 2004.
2. Krauss P., E. A. Rogalla, "Transverse Cracking in Newly Constructed Bridge Decks", NCHRP Report 380, Washington DC, 1996.
3. Curtis R., White H., NYSDOT Bridge Deck Task Force Evaluation of Bridge Deck Cracking on NYSDOT Bridges", NYSDOT, New York, February 2007.
4. Aktan, H., Fu, G., Attanayaka, U., Dekelbab, W., "Investigate Causes and Develop Methods to Minimize Early-age Deck Cracking on Michigan Bridge Decks", Michigan Department of Transportation, 2003.
5. Babaei, K., "Mitigating Transverse Cracking in Concrete Bridge Decks", Transportation Research Board Annual Meeting (CD), Washington, DC, January 2005.
6. Schmitt, T. R., Darwin, D., "Cracking in Concrete Bridge Decks" SM Report No. 39, The University of Kansas Center for Research, Lawrence, Kansas, April 1995.
7. Saadeghvaziri, M. Ala, Hadidi, R., "Cause and Control of Transverse Cracking in Concrete Bridge Decks", New Jersey Department of Transportation, 2002.
8. Brown, M, Sellers, G, Folliard, KJ, Fowler, DW, "Restrained Shrinkage Cracking of Concrete Bridge Decks: State of the Art", Renewed, Report No FHWA/TX-0-4098-1, 2001.
9. Frosch, R.J, Blackman, DT, Radabaugh, R.D, "Investigation of Bridge Deck Cracking in Various Bridge Superstructure Systems", Report No. FHWA/IN/JTRP-2002/25, Indiana Department of Transportation, 2002.
10. Altoubat, S., Lange, D. A., "Creep, Shrinkage, and Cracking of Early Age Concrete Discussion," ACI Materials Journal, Vol. 99, No. 3, 2002.
11. Linford M., Reaveley, L., "Study of the I-15 Reconstruction Project to Investigate Variables Affecting Bridge Deck Cracking", Report UT-04.04, Utah Department of Transportation, 152 pp., 2004.
12. Grasley, Z.C., Lange, D.A., D'Ambrosia, M.D., "Internal Relative Humidity and Drying Gradients in Concrete," Advances in Cement and Concrete, pp. 349, 2003.
13. Wan, B., Foley, C., Komp, J., "Concrete Cracking in New Bridge Decks and Overlays", Transportation Research Centre, Department of Civil and Environmental Engineering, Marquette University, March 2010.
14. Walkowich, T., "Field Monitoring Of Shrinkage Cracking Potential in a High-Performance Concrete Bridge Deck", Rutgers, The State University of New Jersey, January 2011.
15. Eldhose, S., "Simulation of the Long-Term Behavior of Precast/Prestressed Concrete Bridge", Division of Research and Advanced Studies of the University of Cincinnati, March 2006.
16. Qiao, P., Yang, M., McLean, D., "Effect of Intermediate Diaphragms to Prestressed Concrete Bridge Girders in Over-Height Truck Impacts", Washington State Transportation Center (TRAC), WA-RD 696.1, January 2008.
17. Biggs, R. M., Barton, F., Gomez, J., Massarelli, P., McKeel Jr, W., "Finite Element Modeling and Analysis of Reinforced-Concrete Bridge Decks", Virginia Transportation Research Council, Charlottesville, Virginia, September 2000.
18. Minnetyan, L., Janoyan, K., "Tool for Analysis of Early Age Transverse Cracking of Composite Bridge Decks", New York State Department of Transportation, August 2011.

19. Bazant, Z., Baweja, S., “Creep and Shrinkage Prediction Model for Analysis and Design of Concrete Structures: Model B3”, ACI Concrete International, January 2001.
20. Schmitt, T.R., Darwin, D., “Effect of Material Properties on Cracking in Bridge Decks”, Journal of Bridge Engineering, Vol. 4, No. 1, pp. 8-13, 1999.
21. Mindess, S., Young, F., “Concrete”, Prentice-Hall, Inc., Englewood Cliffs, NJ, 1981.
22. Cheng, T. T.-H., Johnston, D. W., “Incidence Assessment of Transverse Cracking in Concrete Bridge Decks: Construction and Material Considerations,” Report No. FHWA/NC/85-002, Vol. 1, North Carolina State University, Raleigh, Department of Civil Engineering, 232 pp. 1985.
23. Holt, E.E., “Early Age Autogenous Shrinkage of Concrete,” Technical Research Centre of Finland, VTT Publications, University of Washington, 2001.
24. Abaqus Version 6.11 Documentation, Abaqus v6.11.
25. ACI COMMITTEE 209 (1992), “Prediction of Creep, Shrinkage and Temperature Effects in Concrete Structures”, Designing for Creep and Shrinkage in Concrete Structures, Publication SP76,193-300, American Concrete Institute, Detroit (1992).
26. AASHTO Standard Specifications for Highway Bridges, 17th Edition (2002). American Association of State Highway and Transportation Officials; Washington DC (2002).
27. Wyffels,T., French,C., Shield,C., ”Effects of Pre-Release Cracks in High-Strength Prestressed Girders”, Report No.2000-25, Department of Civil Engineering University of Minnesota, Minnesota (2000)

APPENDIX

APPENDIX A

Design Example

This design example demonstrates the design of 62.83 ft span AASHTO Type II – I girder as shown below. The superstructure consists of 4 beams spaced at 6’-9” .Beams are designed to act compositely with the 8-in-thick cast-in-place concrete deck slab to resist all superimposed dead loads, live loads, and impact.

Longitudinal Section

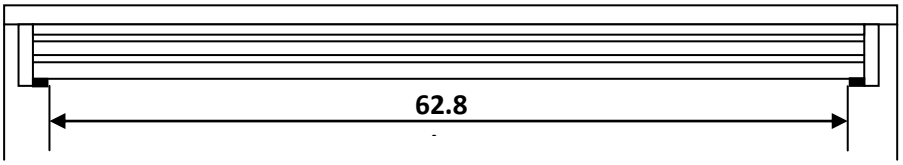

Transverse Cross Section

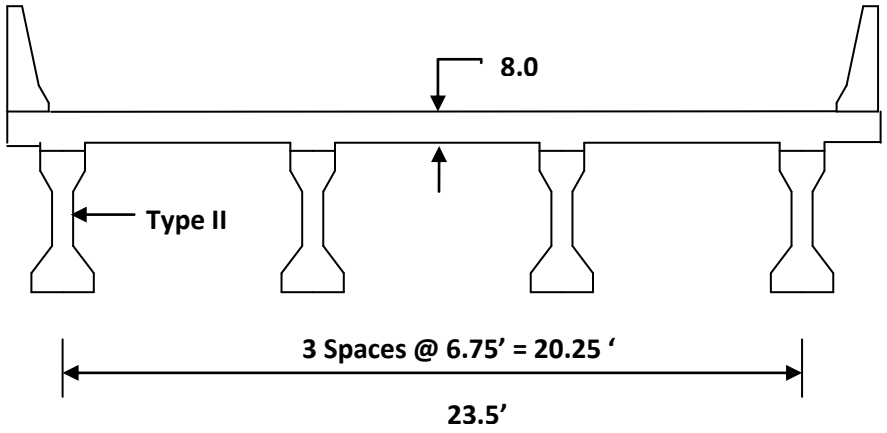

MATERIALS

- Slab

Structural thickness = 8 in; fc’ = 4 ksi

Concrete unit weight, wc = 0.150 kcf

- Precast Beams

AASHTO Type II girder as shown below

fc’ = 7.0 ksi; fci’ = 6.5 ksi

Concrete unit weight, w_c=0.150 kcf

- Prestressing Strand

½ in diameter, low-relaxation

Area of one strand = 0.153 in^2

Ultimate strength, fpu = 270.0 ksi

- Reinforcing Bars

Yield strength, fy = 40 ksi

Modulus of elasticity, Es = 29,000 ksi

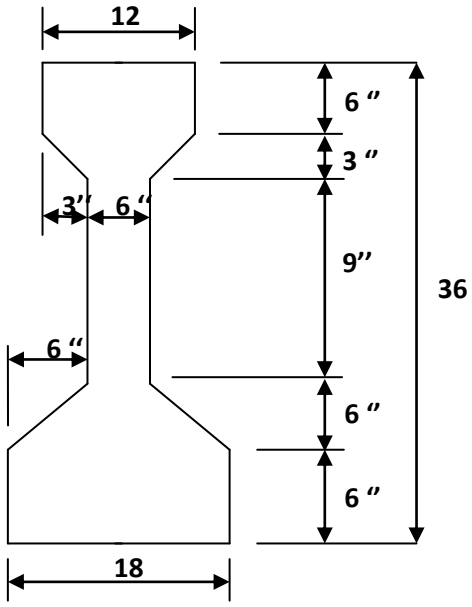

LOADS

Future wearing surface: 0.111 k/ft

Weight of Interior Diaphragms and Diaphragms=0.0398 k/ft

Weight of haunch=0.019 k/ft

Truck: HL 93, including dynamic allowance

CROSSSECTION PROPERTIES FOR A TYPICAL INTERIOR BEAM

- Non-Composite Section

Area (in^2)	369
Weight (lb/ft)	0.384
h (in)	36

y_b (in)	15.83
y_t(in)	20.17
I (in^4)	50980
S_b (in^3)	3220
S_t(in^3)	2527

$E_C = 33000 k_1 w_c^{1.5} \sqrt{f_c'}$ [LRFD 5.4.2.4-1]

$E_C = 33000 \times 1 \times 0.150^{1.5} \times \sqrt{6.5} = 4887.73$ ksi - at transfer

$E_C = 33000 \times 1 \times 0.150^{1.5} \times \sqrt{7} = 5072.24$ ksi - at service loads

- Composite Section

Effective flange Width (1/4) Span = (96.25 ft)(12in/ft)/4 = 188.49 in [LRFD 4.6.2.6]

12ts plus the greater of the web thickness or ½ the beam top flange width:

ts = 8 in (slab thickness - use structural thickness only)

web thickness = 6 in

½ top flange = 0.5(12 in) = 6 in

12(8in) + 6 in = 102 in

Average spacing between beams = 6.75 ft = 81 in (CONTROLS)

- Modular Ratio

n= Ec(slab)/Ec(beam) =4067/5072 =0.8019

- Transformed Section Properties

Transformed flange width = n(effective flange width) = (0.8019)(81) = 64.95 in

Transformed flange area = n(effective flange width)(ts) = (0.8019)(81)(8) = 520 in^2

- Properties of Composite section

Ac (in^2)	889
hc(in)	44
Ic(in^4)	179841
ybc(in)	29.96
ytg(in)	6.04
ytc(in)	14.04
Sbc(in^3)	6003
Stg(in^3)	29775
Stc (in^3)	12809

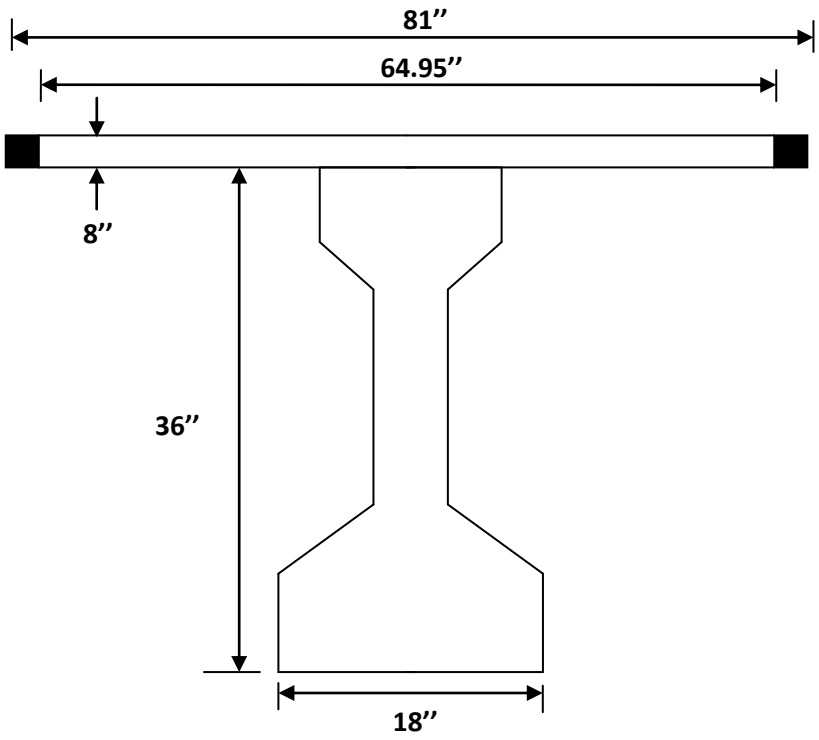

SHEAR FORCES & BENDING MOMENTS

- Dead Loads

Beam Weight: 0.384klf

Slab: (81 in) (8 in) (0.150 kcf)/ (144 in2/ft2) = 0.675klf

Haunch= 0.019klf

Future Wearing Surface=0.111k/f

Diaphragms=0.0398k/ft

Total dead load: 1.2288k/ft

Un factored dead load moment= (1.2288) (62.832)/ (8) =606.3k-ft

- Live Loads

Design truck: HL-93

Load factor: 1.75

Unfactored live load moment= (1.75) (62.832)/ (8) =863.5k-ft

- Distribution Factors

According to LRFD Article 4.6.2.2.1 permanent loads may be distributed uniformly to all beams if the following conditions are met:

Width of deck is constant. OK

Number of beams, $N_b > 4$. OK

Overhang part of the roadway < 3 ft OK

de = 3.25 ft – 1.5 ft = 1.75 ft

Curvature in plan < Specified in Article 4.6.1.2 OK

Cross Section listed in Table 4.6.2.2.1-1 OK

The section meets the criteria.

3.5 <=S<=16.0 S=6.75ft OK

4.5 <=t_s<=12.0 t_s=8 in OK

20<=L<=240 L=62.83 ft OK

N_b>=4 N_b=4 OK

$K_g = n (I+Ae_g^2)$ [LRFD 4.6.2.2.1-1]

n=Ec (beam)/Ec (slab) =5072/4067=1.247

A=369 in^2

I=50980 in^4

e_g=(8/2+2.0+20.17) = 26.17

K_g=1.247 (50980+369*26.17^2) =378,710 in^4

10,000<=K_g<=7,000,000 OK

- Distribution Factors for Bending Moment

For all limit states except for fatigue limit state. [LRFD Table 4.6.2.2.2b-1]

For two or more lanes loaded:

DFM=0.075+(S/9.5)$^{0.6}$+(S/L)$^{0.2}$+ (K_g/12 L*t_s^3)$^{0.1}$

=0.075+ (6.75/9.5)$^{0.6}$ (6.75/62.63)$^{0.2}$ (378710/12/62.83/8^3)$^{0.1}$

=0.595

For one design lane loaded:

DFM=0.06+(S/14)$^{0.4}$+(S/L)$^{0.3}$+ (K_g/12 L*t_s^3)$^{0.1}$

=0.06+ (6.75/14)$^{0.4}$+ (6.75/62.63)$^{0.3}$ (378710/12/62.83/8^3)$^{0.1}$ =0.442

The case of two design lanes loaded controls, DFM = 0.595 lanes/beam

- Distribution Factors for Shear Force

For two or more lanes loaded: [LRFD 4.6.2.2.1-1]

DFV=0.2+(S/12)-(S/35)^2

=0.2+(6.75/12)-(6.75/35)^2

=0.725

For one design lane loaded

DFV=0.36+(S/25)

=0.36+ (6.75/25)

=0.63

The case of two design lanes loaded controls, DFV = 0.725 lanes/beam

- Dynamic Allowance

IM = 33% Where: IM = dynamic load allowance, applied only to truck load

Load Combinations

The following limit states are applicable: [LRFD 3.4.1]

Service I:

Q = 1.00(DC + DW) + 1.00 (LL + IM)

Service III:

Q = 1.00(DC + DW) + 0.80(LL + IM)

Strength I:

Maximum Q = 1.25(DC) + 1.50(DW) + 1.75(LL + IM)

Minimum Q = 0.90(DC) + 0.65(DW) + 1.75(LL + IM)

The initial estimate of number of strands will be found from the Service III combination.

- Service Load Stresses at Mid span

Bottom tensile stress due to applied dead and live loads using load combination Service III:

$F_b = (M_g+M_s/S_b) + (M_b+M_{ws}+ (0.8)\ (M_{LL+I})/S_{bc})$

= ((189.48+362.09)*12/3220) + ((0+54.77+ (0.8) (1.33*863.5))*12/6003)

= 2.05+1.95

= 4 ksi

- Stress Limits for Concrete

According to LRFD Table 5.9.4.2.2-1 the tensile stress limit at service loads is

$Ft=0.19\sqrt{f'c}$

$=0.19*\sqrt{7}$

=0.503 ksi

Required Number of Strands

The difference between the bottom fiber tensile stress due to applied loads and the tensile stress limit is the required precompression stress.

Fpb=fb-ft

=4-0.503

=3.497 ksi

Assume a strand center of gravity at midspan as 8% of the height of the girder.

Ybs=0.08*36

=2.88 in

So the strand eccentricity at the midspan is:

ec= (yb-ybs) =15.83-2.88=12.95 in

If Ppe is the total prestressing force, the stress at the bottom fiber due to prestress is:

fpb=Ppe/A+Ppe ec/Sb

3.497= (Ppe/369) + (Ppe*12.95/3220)

Ppe=506.8 kips

Final prestress force per strand = (area of strand) (fpi) (1-losses, %) where fpi = initial prestressing stress before transfer =0.75 fpu = 202.5 ksi

Assuming 25% loss of prestress the final prestressing force per strand after losses is:

(0.153)(202.5)(1-0.25)=23.2 kips /strand

Number of strands required=506.8/23.2=21.84 strands

Try 28 - ½ in diameter, 270 ksi, low-lax strands.

Strand Pattern

At Mid span

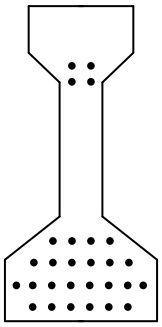

Prestressing Strand Pattern:

No of Strands	Distance from bottom (in)
6	3
8	5
6	7
4	9
2	21
2	23

The distance between the center of gravity of strands and the bottom concrete fiber of the beam ybs is:

ybs = 8.00 in

Strand eccentricity at midspan:

Ec=yb-ybs=15.83-8=7.83 in

At Support

Prestressing Strand Pattern:

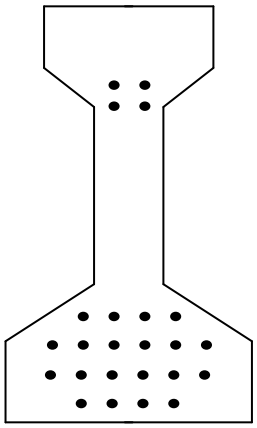

No of starnds	Distance from bottom (in)
4	3
6	5
6	7
4	9
2	21
2	23

4 strands were debonded at the support section to satisfy stress limit requirements

The distance between the center of gravity of strands and the bottom concrete fiber of the beam is, ybs = 8.67 in

Strand eccentricity at midspan:

Ec=yb-ybs=15.83-8.67=7.16 in